Development/Plasticity/Repair

# Opposing Roles for *Hoxa2* and *Hoxb2* in Hindbrain Oligodendrocyte Patterning

**Andrés Miguez,[1,2,3] Sébastien Ducret,[4] Thomas Di Meglio,[4] Carlos Parras,[1,2,3] Hatem Hmidan,[1,2,3] Céline Haton,[1,2,3] Sowmya Sekizar,[1,2,3] Abdelkrim Mannioui,[1,2,3] Marie Vidal,[1,2,3] Aurélien Kerever,[1,2,3] Omar Nyabi,[5] Jody Haigh,[5] Bernard Zalc,[1,2,3,6] Filippo M. Rijli,[4,7] and Jean-Léon Thomas[1,2,3,6,8]**

[1]Université Pierre and Marie Curie–Paris 6, Centre de Recherche de l'Institut du Cerveau et de la Moelle épinière, 75013 Paris, France, [2]Institut National de la Santé et de la Recherche Médicale, Unité Mixte de Recherche S 975, 75013 Paris, France, [3]Centre National de la Recherche Scientifique, Unité Mixte de Recherche 7225, 75013 Paris, France, [4]Friedrich Miescher Institute for Biomedical Research, 4058 Basel, Switzerland, [5]Department for Molecular Biomedical Research, Vlaams Instituut voor Biotechnologie, and Department of Biomedical Molecular Biology, Ghent University, B-9052 Ghent, Belgium, [6]Assistance Publique—Hôpitaux de Paris, Groupe Hospitalier Pitié-Salpêtrière, 75013 Paris, France, [7]University of Basel, CH-4003 Basel, Switzerland, and [8]Yale School of Medicine, Department of Neurology, New Haven, Connecticut 06520-8018

**Oligodendrocytes are the myelin-forming cells of the vertebrate CNS. Little is known about the molecular control of region-specific oligodendrocyte development. Here, we show that oligodendrogenesis in the mouse rostral hindbrain, which is organized in a metameric series of rhombomere-derived (rd) territories, follows a rhombomere-specific pattern, with extensive production of oligodendrocytes in the pontine territory (r4d) and delayed and reduced oligodendrocyte production in the prepontine region (r2d, r3d). We demonstrate that segmental organization of oligodendrocytes is controlled by *Hox* genes, namely *Hoxa2* and *Hoxb2*. Specifically, *Hoxa2* loss of function induced a dorsoventral enlargement of the *Olig2/Nkx2.2*-expressing oligodendrocyte progenitor domain, whereas conditional *Hoxa2* overexpression in the *Olig2*$^+$ domain inhibited oligodendrogenesis throughout the brain. In contrast, *Hoxb2* deletion resulted in a reduction of the pontine oligodendrogenic domain. Compound *Hoxa2*$^{-/-}$*/Hoxb2*$^{-/-}$ mutant mice displayed the phenotype of *Hoxb2*$^{-/-}$ mutants in territories coexpressing *Hoxa2* and *Hoxb2* (rd3, rd4), indicating that *Hoxb2* antagonizes *Hoxa2* during rostral hindbrain oligodendrogenesis. This study provides the first *in vivo* evidence that *Hox* genes determine oligodendrocyte regional identity in the mammalian brain.**

## Introduction

Oligodendrocytes are the myelin-forming cells of the CNS. Despite an apparent similitude of the myelin sheath, oligodendrocytes and their precursors differ by a number of criteria, such as physiological properties, growth-factor dependency, migration pathways, and their different sites of origin along the neural tube (Spassky et al., 1998, 2001; Kessaris et al., 2006; Káradóttir et al., 2008; Tripathi et al., 2011). During development, multiple subpopulations of oligodendrocyte precursor cells (OPCs) are generated in successive waves from different domains along the dorsoventral (DV) axis of the neural tube (Richardson et al., 2006; Rowitch and Kriegstein, 2010). In the spinal cord and hindbrain, OPCs first arise ventrally, adjacent to the midline (Noll and Miller, 1993; Davies and Miller, 2001). In the mouse, the ventral wave of oligodendrogenesis starts at embryonic day (E) 11.5–E13.5 (Timsit et al., 1995; Pringle et al., 1996). From E13.5, additional subpopulations of OPCs develop in the lateral and dorsal plates following a ventrodorsal temporal sequence (Cai et al., 2005; Fogarty et al., 2005; Vallstedt et al., 2005; Sugimori et al., 2007).

The identity of OPCs is determined, at least in part, by the expression of transcription factors, such as Olig1/2, Nkx2.2, or Sox10, that have been characterized along the DV axis of the neural tube (Rowitch, 2004; Wegner, 2008). Dorsally, the Olig2$^+$ domain is abutting the Pax6$^+$ progenitor territory, whereas ventrally it is bordered by the Nkx2.2+ progenitor domain, except in the rostral hindbrain where Olig2$^+$ and Nkx2.2$^+$ progenitor domains almost completely overlap (Vallstedt et al., 2005).

A role for rostrocaudal (RC) positional determinants in oligodendroglial identity has not yet been explored. We have chosen the mouse hindbrain, which is transiently compartmentalized

Received Feb. 23, 2012; revised Oct. 4, 2012; accepted Oct. 5, 2012.

Author contributions: F.M.R. and J.-L.T. designed research; A. Miguez, S.D., T.D.M., C.P., H.H., C.H., S.S., A. Mannioui, and M.V. performed research; A.K., O.N., and J.H. contributed unpublished reagents/analytic tools; A. Miguez and B.Z. analyzed data; A. Miguez, F.M.R., and J.-L.T. wrote the paper.

This work was supported by Institut National de la Santé et de la Recherche Médicale (J.-L.T.), Novartis Research Foundation (F.M.R.), Fédération pour la Recherche sur le Cerveau (J.-L.T., F.M.R.), Fondation pour L'Aide à la Recherche sur la Sclérose En Plaques (J.-L.T., F.M.R., A. Miguez), Agence Nationale Recherche (08-BLAN-0162-01, J.-L.T., C.H.), Swiss National Science Foundation (Sinergia CRSI33_127440) (F.M.R.), Boehringer Ingelheim Fonds (A. Miguez), and Neuroscience pole of research in Ile de France (C.H.). T.D.M. is recipient of a European Molecular Biology Organization long-term fellowship. A. Miguez was a recipient of a grant from a European Cooperation in Science and Technology network while he was working at F.M.R.'s laboratory. We thank D. Rowitch for the gift of the *Olig2-tva-Cre* mouse line. Nkx2.2 and Islet1/2 antibodies, developed by T.M. Jessell and S. Brenner-Morton, and Nkx6.1 antibody, developed by O.D. Madsen, were obtained from the Developmental Studies Hybridoma Bank developed under the auspices of the National Institute of Child Health and Human Development and maintained by the University of Iowa, Department of Biological Sciences, Iowa City, Iowa. Probes for *in situ* hybridization were kindly provided by the following colleagues: D. Rowitch (*Olig1/2*), R. DiLauro (*Nkx2.2*), P. Gruss (*Pax6*), and F. Guillemot (*Ngn2*).

Correspondence should be addressed to any of the following: Dr. Bernard Zalc, Institut National de la Santé et de la Recherche Médicale, Unité Mixte de Recherche S 975, 75013 Paris, France, E-mail: bernard.zalc@upmc.fr; Dr. Filippo M. Rijli, Friedrich Miescher Institute for Biomedical Research, Maulberstrasse 66, 4058 Basel, Switzerland, E-mail: filippo.rijli@fmi.ch; or Dr. Jean-Léon Thomas, Yale School of Medicine, Department of Neurology, New Haven, CT 06520-8018, E-mail: jean-leon.thomas@yale.edu.

DOI:10.1523/JNEUROSCI.0885-12.2012

 0270-6474/12/3217172-14$15.00/0

along the RC axis into seven or eight rhombomeres (r) (Lumsden and Krumlauf, 1996). Hindbrain oligodendrocytes have been the focus of only a few reports describing similarities between hindbrain and spinal cord oligodendrogenesis (Ono et al., 1997; Davies and Miller, 2001; Vallstedt et al., 2005).

*Hox* transcription factors show spatially restricted expression patterns during early neurogenesis and appear as prime candidates as RC positional determinants (Lumsden and Krumlauf, 1996). The *Hox* gene family comprises 39 members, which are organized in four clusters. Each cluster contains a series of paralog genes (*Hox* PG1–*Hox* PG13). *Hox* PG2 genes, namely *Hoxa2* and *Hoxb2*, are activated in neural progenitors during hindbrain segmentation (for review, see Narita and Rijli, 2009). Functional studies in the mouse have shown that *Hox* PG2 genes are involved in the control of rhombomere-specific neuronal patterning, migration, and connectivity (Davenne et al., 1999; Oury et al., 2006; Geisen et al., 2008).

Here, to investigate a possible role of *Hox* PG2 genes in oligodendrogenesis, we focus on the rostral hindbrain, where *Hox* PG2 genes display their main patterning role (Narita and Rijli, 2009). We provide *in vivo* evidence that *Hox* PG2 genes confer an RC segmental identity to rostral hindbrain OPCs. Moreover, we found that *Hoxa2* and *Hoxb2* have opposing roles, namely repressing and promoting oligodendrogenesis, respectively. These findings indicate that a tight regulation of the balance between *Hox* PG2 gene activities is required for proper RC oligodendrocyte patterning in the rostral hindbrain.

## Materials and Methods

*Generation of the ROSA::(lox-STOP-lox)Hoxa2-IRES-EGFP mouse line.* The conditional Hoxa2 overexpression mouse line was generated by using the Gateway-compatible *ROSA26* locus targeting vector as previously described (Nyabi et al., 2009). LR reactions were performed between the plasmid pENTR-FLAG-Hoxa2 (containing the Hoxa2 cDNA coding sequence with a 5′FLAG tag) and the destination vector pROSA26-DV1 to obtain the targeting vector pROSA26-FLAG-Hoxa2-IRES-EGFP. This vector was linearized with PvuI and electroporated into the E14 embryonic stem (ES) cell line. The positive ES cell clones, selected by G418 resistance and screened by PCR, were aggregated with morula-stage embryos obtained from inbred (C57BL/6 × DBA/2) F1 mice. Germline transmission of the *ROSA26::(lox-STOP-lox)Hoxa2-IRES-EGFP* allele was obtained. Heterozygous and homozygous mice were viable and fertile.

*Generation of a conditional* Hoxb2 *mutant allele and* Hoxb2*-null mouse line.* To generate a *Hoxb2* mutant allele suitable for conditional knockout studies, we used a strategy based on both Cre-mediated (Gu et al., 1993) and Flp-mediated (Dymecki, 1996) recombination to generate a selection marker-free locus flanked by recombinase-specific sites. A *neo*-cassette driven by the phosphoglycerate kinase (PGK) promoter was inserted in the *Hoxb2* intron, 950 bp downstream of the translational start codon. The PGK-*neo* cassette was flanked by two *Frt* sites for Flp-mediated excision and a *loxP* site immediately following the 3′ *Frt* site. A second *loxP* site was also introduced in the *Hoxb2* 3′UTR, 468 bp downstream of the *Hoxb2* translational stop codon, for Cre-mediated conditional deletion. Thus, neither the *loxP* sites nor the *Frt*-flanked PGK-*neo* cassette interrupted the *Hoxb2* coding sequence. Homologous recombination of the targeting vector was obtained in ES cells and confirmed by Southern blot, PCR, and sequencing analysis. Germline transmission of the *Hoxb2(Frt-neo-Frt)lox* allele was obtained, and heterozygous mutant mice were viable and fertile. *In vivo* Flp-mediated excision of the PGK-*neo* cassette was obtained by mating the $Hoxb2^{(Frt\text{-}neo\text{-}Frt)lox}$ allele to the ACTB:FLPe deleter to obtain the $Hoxb2^{flox}$ allele (Rodríguez et al., 2000). Following germline transmission of the $Hoxb2^{flox}$ allele to the progeny, correct excision of the selection marker cassette was confirmed by PCR and sequencing. $Hoxb2^{flox/+}$ and $Hoxb2^{flox/flox}$ mutant mice were produced at Mendelian frequency, had no obvious abnormalities, were fertile, and survived a normal lifespan. To obtain a *Hoxb2*-null allele, a *CMV::Cre* transgenic deleter (Dup é et al., 1997) was mated to $Hoxb2^{flox/+}$ mutant mice. The ensuing $Hoxb2^{del/+}$ progeny had no obvious abnormalities, were fertile, and survived a normal lifespan. $Hoxb2^{del/del}$ homozygous-null mutants were generated by crossing $Hoxb2^{del/+}$ heterozygotes.

*Generation of* Hoxa2/Hoxb2*-deficient mice.* $Hoxb2^{del/+}$ mice were crossed with $Hoxa2^{EGFP+/-}$ mice to obtain double heterozygous mutant animals. $Hoxb2^{del/+}$;$Hoxa2^{EGFP+/-}$ mice were mated to obtain *Hoxa2/Hoxb2* homozygous-null mutants.

*Mouse strains, tamoxifen treatment, and genotyping.* OF1 wild-type mice were obtained from Charles River. The following mouse strains were used: $Hoxa2^{EGFP(lox\text{-}neo\text{-}lox)}$, $Hoxa2^{EGFP+/-}$, and $Hoxa2^{flox}$ (Pasqualetti et al., 2002; Ren et al., 2002); *CMV-βactin-CreERT2* (Santagati et al., 2005); *Olig2-tva-Cre* (Schüller et al., 2008; gift from D. Rowitch, University of California, San Francisco). For tamoxifen (Tx) treatments, Tx was provided by oral gavage (10 mg/30–40 g of body weight) into pregnant mice at day 10.5 of gestation, according to Santagati et al. (2005). All genotypes were confirmed by PCR of tail DNA using specific primers. Noon of the plug day was considered as E0.5 and mice of either sex were used. All animal studies were performed in accordance with the guidelines issued by the French Ministry of Agriculture and Swiss cantonal authorities.

*Reagents.* Antibodies used were anti-Pax6 (polyclonal rabbit, 1:500, Covance), anti-Olig2 (polyclonal rabbit, 1:200, Millipore), anti-Nkx2.2 [monoclonal mouse, 1:2, Developmental Studies Hybridoma Bank (DSHB)], anti-Nkx6.1 (mouse, 1:400, DSHB), anti-Islet 1:2 (mouse, 1:200, DSHB), anti-PDGF receptor α (anti-PDGFRα) (rat, 1:400, BD Biosciences), anti-phospho-histone 3 (mouse, 1:500, Millipore), anti-GFP (chick, 1:2000, Aves Labs), anti-CNPase (mouse, 1:500, Millipore), anti-5HT (rabbit, 1:1000, Sigma-Aldrich), anti-Sox9 (rabbit, 1:1000, gift from M. Wegner), anti-Sox10 (guinea pig, 1:1000, gift from M. Wegner), anti-Pax3 (mouse, 1:100, gift from F. Relaix), anti-Pax7 (mouse, 1:10, gift from F. Relaix), and anti-O4 (mouse, 1:4, gift from I. Sommer). Fluorescent secondary antibodies were Alexa Fluor 488, Alexa Fluor 594, and Alexa Fluor 647 Ig (1:1000, Invitrogen). *Hoxa2* and *Hoxb2* riboprobes were previously described (Hunt et al., 1991).

*Immunohistochemistry and* in situ *hybridization.* Embryonic brains were fixed by immersion in 4% paraformaldehyde in 0.12 M phosphate buffer, pH 7.4 (PFA). Brain cryosections were blocked in 10% fetal bovine serum in PBS containing 0.3% Triton X-100 and incubated overnight at room temperature with primary antibodies, followed by species-specific secondary antibodies. Whole hindbrain explants were dissected out in a PBS/0.6% glucose solution, opened dorsally, and fixed in PBS containing 4% PFA before immunostaining. For cryosections, cell nuclei were stained by incubation with Hoechst and slides were mounted with Fluoromount (Southern Biotechnologies Associates). Hindbrain explants were mounted with ProLong (Invitrogen). *In situ* hybridizations were performed as described in Spassky et al. (1998).

*Image acquisition and quantifications.* Image acquisition was performed using a fluorescence macroscope (MacroFluo Z6/Z16 APO, Leica), a fluorescence microscope equipped with the apotome system (AxioImager Z1, Zeiss), and a brightfield microscope equipped with a CCD camera (DFC 360FX/420C, Leica). The size of the Olig2 ventricular domain on hindbrain flat-mounts was measured using ImageJ software for digital tracing. The number of ventral $Olig2^+$ and $PDGFR\alpha^+$ cells on sagittal cryosections was evaluated as the average number of labeled cells counted on five successive sagittal sections (20 μm each) on one side of the floor plate (see Figs. 3, 4, 6). The number of $PH3^+$ and $PH3^+$/$PDGFR\alpha^+$ cells were counted similarly. The number of ventral $PDGFR\alpha^+$ cells in the forebrain was counted on six successive coronal sections (overall thickness, 300 μm) in the anterior entopeduncular area/medial ganglionic eminence region (see Fig. 3). The percentage of $Olig2^+$ migrating cells (see Figs. 3, 6) was calculated with Prism software by comparing integrated intensity of the migrating zone with that of the ventricular zone, as previously described (Di Lullo et al., 2011).

*Statistical analyses.* GraphPad Prism software was used for statistical analysis. Data were compared using Student's *t* test, unless otherwise specified. Significant *p* values are indicated in figure legends. All error bars represent SEM.

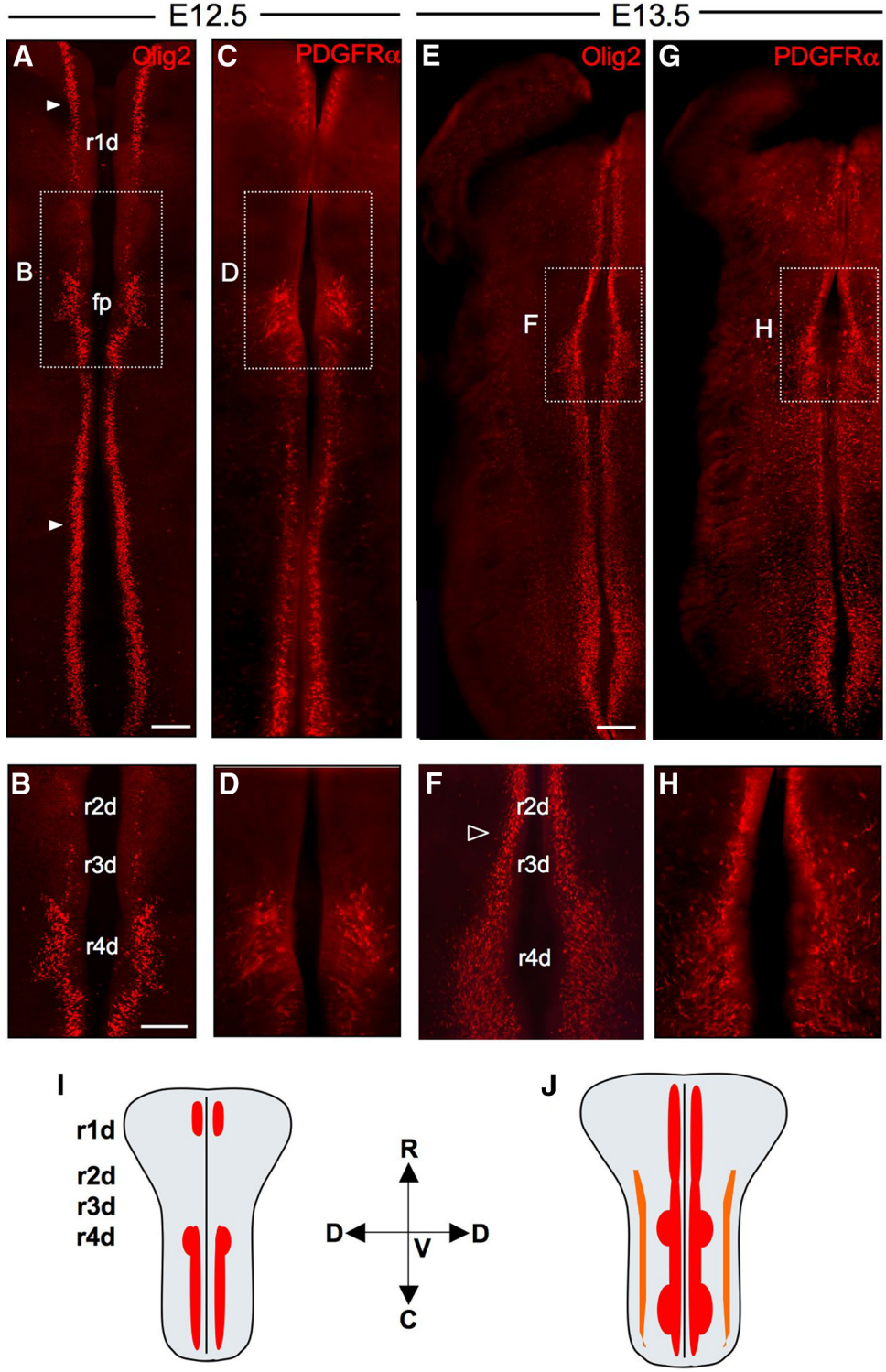


**Figure 1.** Segmental pattern of oligodendrogenesis in the developing hindbrain. Hindbrain flat-mounts from E12.5 and E13.5 wild-type embryos labeled for Olig2 and PDGFR$\alpha$. ***A–D***, At E12.5, ventral Olig2-expressing and PDGFR$\alpha$-expressing cells are found at the rhombomesencephalic boundary (r1d), rare or absent in r2d-r3d domains, expanded in r4d, and, from r5d, they form two bilateral columns extending toward the spinal cord. ***E–H***, From E13.5 onwards, both ventral and dorsal (not visible at low magnification) pools of Olig2$^+$/PDGFR$\alpha^+$ cells extend along the entire rostrocaudal length of the hindbrain. ***I***, ***J***, Schematic representation of flat-mounted hindbrains showing the spatiotemporal pattern of oligodendrogenesis at E12.5 (***I***) and E13.5 (***J***), with both ventral (red) and dorsal (orange) pools of OPCs. R, Rostral; C, caudal; V, ventral; D, dorsal; r(*n*)d, rhombomere-derived domain; fp, floor plate. Scale bars: ***A, C, E, G***, 300 $\mu$m; ***B, D, F, H***, 100 $\mu$m.

## Results

### Segmental pattern of oligodendrogenesis in the developing hindbrain

We set out to study the onset of hindbrain oligodendrogenesis with antibodies against Olig2 and PDGFR$\alpha$, which are early markers of oligodendrocyte lineage (Rowitch, 2004). Flat-mount hindbrain preparations were examined at developmental stages E12.5 and E13.5 (i.e., when the first hindbrain OPCs arise) (Vallstedt et al., 2005). At E12.5, Olig2$^+$ cells showed a bilateral and discontinuous pattern of distribution in the ventral neuroepithelium. Along the RC

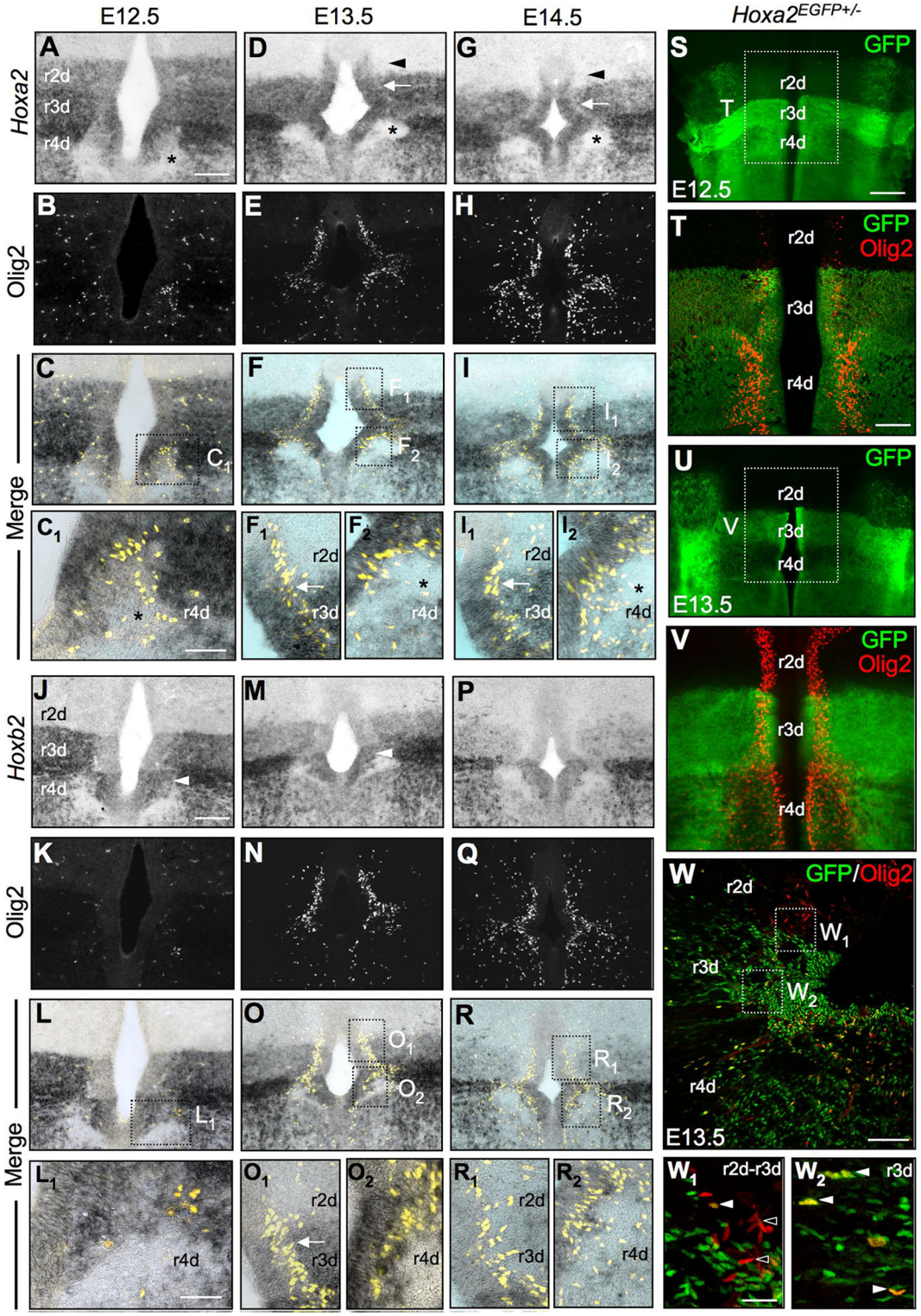


**Figure 2.** *Hox* PG2 expression in the *Olig2* domain of the developing rostral hindbrain. ***A–R***, Hindbrain coronal cryosections from E12.5–E14.5 wild-type embryos at the r2d-r4d level, double labeled with anti-Olig2 antibody and an antisense riboprobe specific for *Hoxa2* (***A–I***) and *Hoxb2* (***J–R***) transcripts (Fig. 7*F*, position of section plan on a lateral view of hindbrain). ***A–F***, From E12.5 to E13.5, *Hoxa2* expression is downregulated in the prepontine r2d region, especially in the parenchyma (***D,*** arrowhead), correlating with the extension of Olig2 expression in this domain. ***G–I***, From E13.5 to E14.5, *Hoxa2* expression regresses in the prepontine and pontine regions, especially in r2d (***G,*** arrowhead) and r4d, while Olig2 $^{+}$ cells expand in these domains. At all developmental stages examined, Olig2 $^{+}$ cells form among *Hoxa2*-expressing progenitors, but they concentrate at the external edge of ventricular domain (***B***, ***E***, ***H***) and within territories where *Hoxa2* expression is downregulated (***D, G, F$_1$, I$_1$,*** arrows). ***C$_1$, F$_1$, F$_2$, I$_1$, I$_2$***, High magnifications of frames in ***C***, ***F***, and ***I***. Olig2 $^{+}$ cells include both *Hoxa2*-expressing cells in the ventricular layer (***I$_2$***) and *Hoxa2*-negative cells, which are predominantly OPCs migrating in the subventricular layer and descending axonal tracts (***C$_1$, F$_2$, I$_2$***). Asterisks in ***D***, ***G***, ***C$_1$***, ***F$_2$,*** and ***I$_2$*** indicate descending axonal tracts. ***J–R***, *Hoxb2* transcripts were not detected in the r2d territory and showed the highest level of expression in r4d (***J***, ***M***, ***P***). Arrowheads in ***J*** and ***M*** indicate the lateral extension of the *Hoxb2*-expressing ventricular domain in r4d. ***K–R***, Olig2 $^{+}$ cells include few *Hoxb2*-expressing cells, especially localized in the ventricular layer of r4d (***L$_1$***, ***O***, ***O$_1$***, ***O$_2$***), but mainly concentrate at the external ventricular edge where *Hoxb2* expression is downregulated (***O$_1$,*** arrow). The majority of migrating OPCs do not express *Hoxb2* at E13.5 and E14.5 (***R***, ***R$_1$***, ***R$_2$***). ***L$_1$***, ***O$_1$***, ***O$_2$***, ***R$_1$***, ***R$_2$***, High magnifications of frames in ***L***, ***O***, and ***R***. ***S–V***, Hindbrain flat-mounts from *Hoxa2$^{EGFP+/-}$* embryos double labeled with antibodies against GFP (green) and Olig2 (red). From E12.5 to E13.5, the level (*Figure legend continues.*)

axis, Olig2$^+$ cells localized at the rhombomesencephalic boundary (rld) were rare or absent in r2d-r3d domains, expanded dorsoventrally in the r4d domain, which corresponds to the presumptive pontine region, and from the r5d territory formed two bilateral columns extending toward the spinal cord (Fig. 1*A*,*B*). At E13.5, the Olig2-expressing domain had become continuous along the ventral hindbrain, although still larger in r4d than in r2d-r3d (Fig. 1*E*,*F*). A similar spatiotemporal pattern of expression was displayed by other specific oligodendroglial markers, such as PDGFRα (Fig. 1*C*,*D*,*G*,*H*), Sox10, *Olig1*, and O4 (data not shown). Therefore, between E12.5 and E13.5, oligodendrocytes form in the rostral hindbrain with rhombomere-specific patterns, with a 1 d delay in r2d-r3d and in larger number in r4d.

### *Hox* PG2 expression in the *Olig2* domain of the developing rostral hindbrain

Among *Hox* family members, *Hox* PG2 genes display the rostralmost expression domains in the CNS. Along the hindbrain RC axis, *Hoxa2* and *Hoxb2* have overlapping expression domains with offset rostral boundaries mapping in r2 and r3 for *Hoxa2* and *Hoxb2*, respectively. Moreover, progenitors along the DV axis display distinct *Hoxa2* and *Hoxb2* expression levels (Davenne et al., 1999).

We compared *Hoxa2* and Olig2 expression in the rostral hindbrain from E12.5 to E14.5, first on coronal cryosections double labeled with anti-Olig2 antibody and an antisense riboprobe specific for *Hoxa2* transcripts. We observed that (1) *Hoxa2* expression is progressively downregulated in the prepontine r2d region (Fig. 2*A*,*D*,*G*, arrowheads in *D* and *G*), while Olig2 expression extends into this domain (Fig. 2*B*,*C*,*E*,*F*,*H*,*I*); (2) Olig2$^+$ cells appear at the dorsal edge of the ventricular progenitor domain in r3d-r4d (Fig. 2*B*,*C*,*E*,*F*,*H*,*I*) and localize in low-expressing *Hoxa2*$^+$ sites, while the ventricular domain expresses fairly high *Hoxa2* transcript levels (Fig. 2$F_1$,$I_1$, arrows); and (3) Olig2$^+$ cells migrate through territories where *Hoxa2* expression is downregulated, such as in the descending axonal tracts in r4d (Fig. 2$C_1$,$F_2$,$I_2$, asterisks).

We next analyzed the expression pattern of *Olig2* in *Hoxa2*$^{EGFP+/-}$ mice, which express the *EGFP* knocked-in at the *Hoxa2* locus, thus faithfully mimicking the endogenous *Hoxa2* expression pattern (Pasqualetti et al., 2002). Hindbrain flat-mounts from *Hoxa2*$^{EGFP+/-}$ embryos were double labeled with antibodies against GFP and Olig2. From E12.5 to E13.5, bilateral columns of Olig2$^+$ cells emerged at the dorsal edge of the ventralmost GFP$^+$ progenitor domain (i.e., the *Hoxa2*$^+$/*Nkx2.2*$^+$ domain) in r3d-r4d, while GFP expression levels decreased in the ventral and alar plates of r2d, similar to the distribution of endogenous *Hoxa2* transcripts (Fig. 2*S*–*V*). At the cellular level, more ventricular Olig2$^+$ cells expressed GFP in the r3d than in the r2d domain (Fig. 2$W_1$,$W_2$). At E18.5, EGFP expression was expressed by the majority of CNP$^+$ mature oligodendrocytes in prepontine and pontine territories (data not shown). Altogether, these data indicate that low levels of *Hoxa2* expression correlate with the expansion of Olig2$^+$ progenitors at the onset of oligodendrogenesis.

Next, we compared the expression of Olig2 with that of the other *Hox* PG2 gene, *Hoxb2*. Coronal cryosections of hindbrain, at developmental stages E12.5, E13.5, and E14.5, were colabeled with anti-Olig2 antibody and an antisense riboprobe against *Hoxb2* (Fig. 2*J*–*R*). *Hoxb2* transcripts were not detected in the r2d territory, as expected from its normal expression domain. *Hoxb2* and *Hoxa2* were both expressed in r3d as well as in r4d, which showed the highest level of *Hoxb2* expression (Fig. 2*J*,*M*,*P*). Notably, *Hoxb2* expression expanded dorsally in the r4d *Nkx2.2*$^+$ domain, where Olig2$^+$ cells colocalized with *Hoxb2*-expressing progenitors, especially at E12.5–E13.5 and unlike *Hoxa2* (Fig. 2*J*,*M*, arrowheads; Fig. 2$O$–$O_2$; Davenne et al., 1999). In contrast, the majority of migrating OPCs did not appear to express *Hoxb2* at E13.5 and E14.5 (Fig. 2*O*,*R*).

Altogether, the spatiotemporal patterns of *Hoxa2* and *Hoxb2* expression between E12.5 and E14.5 suggest their potential involvement in segment-specific patterning of the ventral *Olig2*$^+$ oligodendrocyte subpopulation.

### Conditional *Hoxa2* overexpression in *Olig2*$^+$ cells inhibits oligodendrogenesis

In the rostral hindbrain, *Hoxa2* is expressed at low levels in *Olig2*$^+$ progenitors at the onset of oligodendrogenesis (Fig. 2*C*,*F*). Thus, one possibility is that downregulation of *Hoxa2* is a prerequisite to allow the appearance of *Olig2* expression at the dorsal edge of the Nkx2.2$^+$ domain and, in turn, to induce ventral oligodendrocyte generation. We therefore examined whether forced *Hoxa2* overexpression in *Olig2*$^+$ progenitors could inhibit hindbrain oligodendrogenesis. Conditional *Hoxa2* overexpression was induced by mating the *Olig2-tva-Cre* line (Schüller et al., 2008) with a newly generated allele *ROSA26::(lox-STOP-lox)Hoxa2-IRES-EGFP* (hereafter referred to as *Olig2-tva-Cre*;*ROSA*$^{(lox\text{-}stop\text{-}lox)Hoxa2}$ mice), in which *Hoxa2* is selectively activated only in the *Olig2* lineage upon Cre-mediated recombination (see Materials and Methods). Hindbrain flat-mounts from E13.5 *Olig2-tva-Cre*;*ROSA*$^{(lox\text{-}stop\text{-}lox)Hoxa2}$ embryos were immunostained to detect oligodendroglial cells with antibodies against Olig2 and PDGFRα. The dorsoventral extent of the Olig2$^+$ ventricular domain was reduced in the r2d-r3d region, compared with *ROSA*$^{(lox\text{-}stop\text{-}lox)Hoxa2}$ controls (Fig. 3*A*,*C*,*D*,*F*,*G*). Quantification of the number of PDGFRα$^+$ OPCs on sagittal sections confirmed that, in these conditional *Hoxa2* gain-of-function mutants, ventral oligodendrogenesis was decreased by ~2-fold in the prepontine and pontine territories (r2d-r4d) (Fig. 3*B*,*C*,*E*,*F*,*H*). Therefore, forced *Hoxa2* expression in Olig2$^+$ cells inhibits ventral hindbrain oligodendrogenesis.

Remarkably, the Olig2$^+$/PDGFRα$^+$ cell population was also reduced by ~50% in *Olig2-tva-Cre*;*ROSA*$^{(lox\text{-}stop\text{-}lox)Hoxa2}$ embryos compared with controls in ectopic brain territories where *Hoxa2* is not normally expressed during development, such as the ventral forebrain [Fig. 3*L*–*O*; mean number of PDGFRα$^+$ cells per area (mm$^2$) ± SEM: *ROSA*$^{(lox\text{-}stop\text{-}lox)Hoxa2}$, 156.4 ± 6.91; *Olig2-tva-Cre*;*ROSA*$^{(lox\text{-}stop\text{-}lox)Hoxa2}$, 81.76 ± 5.56; $p < 0.0001$, Student's *t* test, $n = 3$]. As shown in Figure 3*P*–*R*, EGFP, which is directly translated from the IRES of the allele overexpressing *Hoxa2* (see Materials and Methods), and Olig2 expression levels are inversely correlated in ventricular forebrain progenitors. Namely, Olig2 levels are low in ectopic *EGFP/Hoxa2* highly expressing cells (Fig. 3*Q*,*R*, dark arrowheads), while progenitors strongly expressing Olig2 display low levels of *EGFP/Hoxa2* ecto-

←

(*Figure legend continued.*) of *Hoxa2/EGFP* expression decreases in the basal plate of r2d and r4d (***S***, ***U***), while bilateral columns of Olig2$^+$ cells enlarge in these domains (***T***, ***V***). *Hoxa2*/EGFP expression is maintained in the ventralmost ventricular domain of r3d. ***W***, Sagittal section of a *Hoxa2*$^{EGFP+/-}$ E13.5 embryo at the r2d-r4d level, labeled for GFP (green) and Olig2 (red). Ventricular Olig2$^+$ cells expressing *Hoxa2*/EGFP were detected in r3d-r4d, but not in r2d. In the subventricular layer of r2d-r4d region, both Olig2$^+$EGFP$^-$ (dark arrowheads) and Olig2$^+$EGFP$^+$ (white arrowheads) cells were observed, and the majority of Olig2$^+$ cells migrating in the parenchyma were GFP$^+$ (***W*$_1$**, ***W*$_2$**). r(*n*)d, rhombomere-derived domain. Scale bars: ***S***, ***U***, 200 μm; ***A*--*I***, ***J*--*R***, ***T***, ***V***, ***W***, 100 μm; ***C*$_1$**, ***F*$_1$**, ***F*$_2$**, ***I*$_1$**, ***I*$_2$**, ***L*$_1$**, ***O*$_1$**, ***O*$_2$**, ***R*$_1$**, ***R*$_2$**, 50 μm; ***W*$_1$**, ***W*$_2$**, 25 μm.

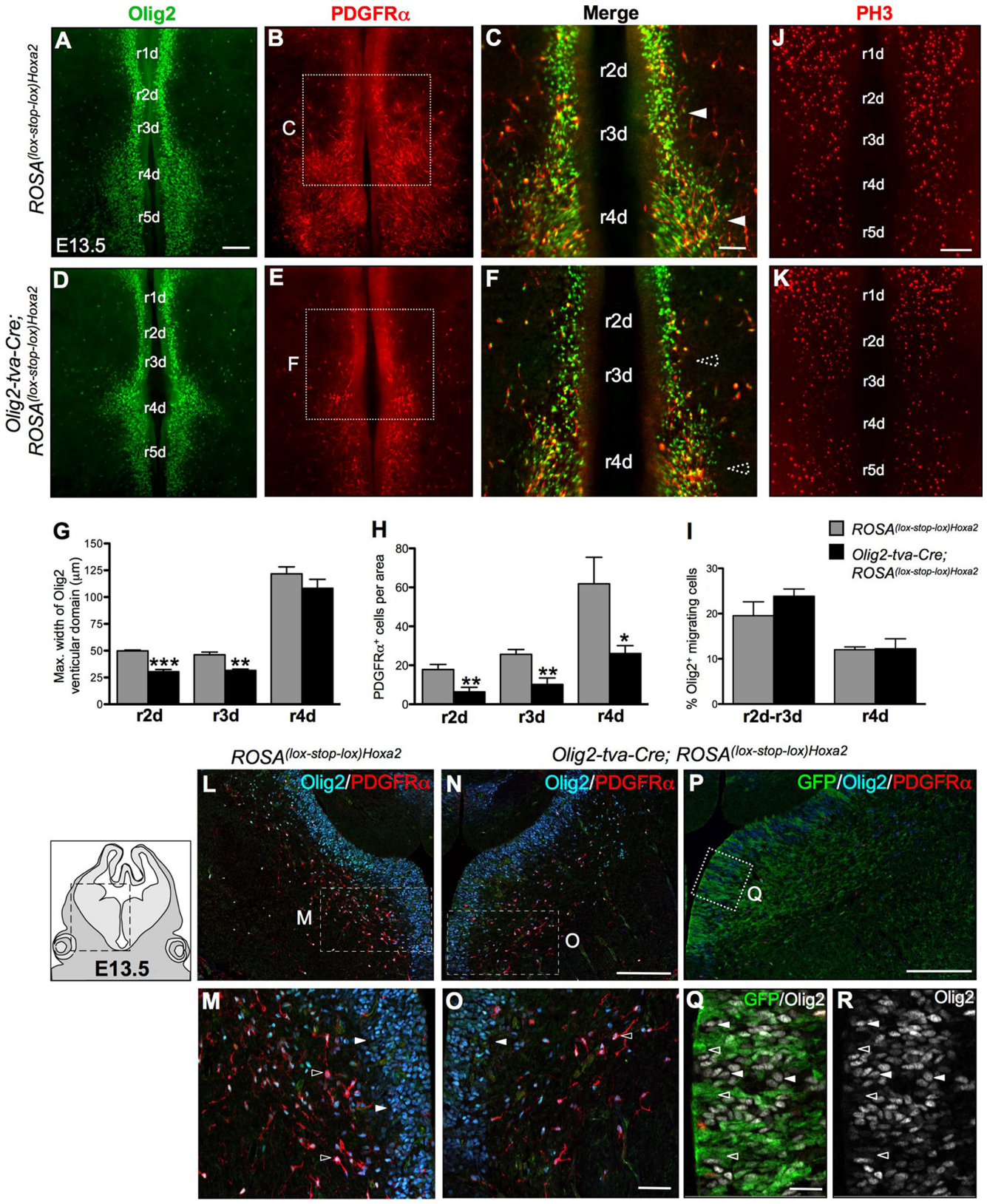


**Figure 3.** Conditional *Hoxa2* overexpression in *Olig2*$^+$ cells inhibits oligodendrogenesis. ***A–I***, Hindbrain flat-mounts from *ROSA*$^{(lox\text{-}stop\text{-}lox)Hoxa2}$ (***A–C***) and *Olig2-tva-Cre*; *ROSA*$^{(lox\text{-}stop\text{-}lox)Hoxa2}$ (***D–F***) embryos at E13.5, labeled for Olig2 (green) and PDGFRα (red). *Hoxa2* gain of function in *Olig2*-expressing cells results in a reduced Olig2$^+$ progenitor domain in r2d and r3d (***A***, ***C***, ***D***, ***F***, ***G***) and a decreased number of PDGFRα$^+$ cells in the basal plate of r2d, r3d, and r4d (***B***, ***C***, ***E***, ***F***, ***H***). No differences between genotypes were found regarding the percentage of Olig2$^+$ migrating cells (***I***). ***J***, ***K***, Hindbrain flat-mounts labeled for PH3, showing that *Olig2-tva-Cre*; *ROSA*$^{(lox\text{-}stop\text{-}lox)Hoxa2}$ embryos display a decreased number of PH3$^+$ proliferating cells, compared with control animals. ***L–R***, Coronal sections from *ROSA*$^{(lox\text{-}stop\text{-}lox)Hoxa2}$ (***L***, ***M***) and *Olig2-tva-Cre*; *ROSA*$^{(lox\text{-}stop\text{-}lox)Hoxa2}$ (***N–R***) E13.5 embryos, at the level of the anterior entopeduncular area/medial ganglionic eminence of the forebrain, labeled for Olig2 (blue), PDGFRα (red), and GFP (green). ***M***, ***O***, The number of Olig2$^+$ (white arrowheads) and PDGFRα$^+$ (black arrowheads) in *Olig2-tva-Cre*; *ROSA*$^{(lox\text{-}stop\text{-}lox)Hoxa2}$ embryos was reduced by half compared with controls. High levels of *EGFP/Hoxa2* and *Olig2* expression were mutually exclusive in ventricular progenitors (***P***). ***Q***, (*Figure legend continues.*)

pic expression (Fig. 3*Q*,*R*, white arrowheads). Thus, *Hoxa2* can inhibit *Olig2* expression in a cell-autonomous manner in progenitor cells throughout the brain.

We next analyzed the migration and proliferation of OPCs in hindbrain flat-mounts of E13.5 *Hoxa2*-gain-of-function mutants. At this stage, the Olig2$^+$ ventricular zone is observed as two bilateral columns of dense populations of cells next to the ventral midline, while Olig2$^+$ migrating cells disperse laterally in the ventroalar plate (Fig. 3*A*,*D*). We quantified the ratio of migrating versus ventricular/nonmigrating progenitors as a function of fluorescence intensity in respective areas, as previously reported (Di Lullo et al., 2011). Figure 3*I* quantifies the percentage of cells located in the migration area of the r2d-r3d and r4d domains. The percentage of migrating Olig2$^+$ cells was similar between *Olig2-tva-Cre*;*ROSA*$^{(lox\text{-}stop\text{-}lox)Hoxa2}$ gain-of-function mutants and *ROSA*$^{(lox\text{-}stop\text{-}lox)Hoxa2}$ controls, suggesting that OPCs' migratory properties were not altered by *Hoxa2* forced expression. In contrast, cell proliferation was reduced in the ventroalar plate of r2d-r4d, as shown by immunolabeling of hindbrain flat-mounts (Fig. 3*J*,*K*) and sagittal sections with anti-phospho-histone H3 (PH3) antibody. *Hoxa2* overexpression induced a decrease in the number of PH3$^+$ cells [mean number of PH3$^+$ cells per area (mm$^2$) ± SEM: *ROSA*$^{(lox\text{-}stop\text{-}lox)Hoxa2}$ (control), 35.7 ± 1.9, *Olig2-tva-Cre*;*ROSA*$^{(lox\text{-}stop\text{-}lox)Hoxa2}$: 14.8 ± 1.8, $p = 0.0004$; Student's *t* test, $n = 3$], and less OPC proliferation (percentage of PH3$^+$/PDGFRα$^+$ cells/total PDGFRα$^+$ cells ± SEM: *ROSA*$^{(lox\text{-}stop\text{-}lox)Hoxa2}$, 7.1 ± 1.2, *Olig2-tva-Cre*;*ROSA*$^{(lox\text{-}stop\text{-}lox)Hoxa2}$, 3.1 ± 0.4, $p = 0.0346$; Student's *t* test, $n = 3$). These data suggest that *Hoxa2* has a primary effect on the generation rather than on the migration of OPCs.

Finally, we investigated whether the reduced oligodendrogenesis induced by *Hoxa2*-overexpression resulted in an alteration of hindbrain oligodendrocyte population at later stages of development. We quantified OPCs (PDGFRα$^+$) as well as cells expressing 2-cyclic nucleotide 3-phosphodiesterase (CNP), a marker for differentiated oligodendrocytes (Kim et al., 1984), on sagittal sections of hindbrain at E18.5. The number of OPCs and mature oligodendrocytes in *Hoxa2*-gain-of-function mutants and controls were similar [mean number of PDGFRα$^+$ cells per area (mm$^2$) ± SEM: r2d: *ROSA*$^{(lox\text{-}stop\text{-}lox)Hoxa2}$ (control), 265.2 ± 78.4; *Olig2-tva-Cre*;*ROSA*$^{(lox\text{-}stop\text{-}lox)Hoxa2}$, 319.8 ± 94.1; r3d: *ROSA*$^{(lox\text{-}stop\text{-}lox)Hoxa2}$, 360.7 ± 132.2; *Olig2-tva-Cre*;*ROSA*$^{(lox\text{-}stop\text{-}lox)Hoxa2}$, 419.3 ± 134.7; mean number of CNP$^+$ cells per area (mm$^2$): r2d: *ROSA*$^{(lox\text{-}stop\text{-}lox)Hoxa2}$, 9.1 ± 7.6; *Olig2-tva-Cre*;*ROSA*$^{(lox\text{-}stop\text{-}lox)Hoxa2}$, 12.9 ± 14.5; r3d: *ROSA*$^{(lox\text{-}stop\text{-}lox)Hoxa2}$, 9.5 ± 10.9; *Olig2-tva-Cre*;*ROSA*$^{(lox\text{-}stop\text{-}lox)Hoxa2}$, 30.6 ± 37.8; $n = 3$]. These data suggest that the reduced oligodendrogenesis observed at E13.5 is compensated at later stages, either by additional proliferation or by increased survival of OPCs. In *Hoxa2-GOF* mutants, there is less competition between the remaining ventral OPCs for growth factors, such as PDGF-A, which determines the final number and distribution of mature oligodendrocytes (Calver et al., 1998), and OPCs may expand transiently more rapidly. We have tested this hypothesis at embryonic stage E16.5, between the onset of oligodendrogenesis (E12.5) and the onset of oligodendrocyte differentiation (E17.5–E18.5). We found that *Hoxa2-GOF* mutants showed more proliferating OPCs in the prepontine domain than control embryos [percentage of PH3$^+$/PDGFRα$^+$ cells/total PDGFRα$^+$ cells per section ± SEM (r2d-r3d): *Olig2-tva-Cre*; *ROSA*$^{(lox\text{-}stop\text{-}lox)Hoxa2}$, 8.5 ± 0.3; *ROSA*$^{(lox\text{-}stop\text{-}lox)Hoxa2}$, 5.8 ± 0.2; $p = 0.0152$, Student's *t* test, 3 sections/embryo, $n = 3$]. Additional immunostaining for cleaved caspase-3 to detect cells undergoing apoptosis in the r2d-r3d domain revealed caspase-3$^+$ cells, but failed to show caspase-3$^+$/PDGFRα$^+$ cells both in controls and *Hoxa2*-gain-of-function mutants (data not shown), suggesting that OPC survival is likely not affected by *Hoxa2* overexpression. Thus, the twofold reduction in ventricular progenitors observed in *Hoxa2-GOF* is rapidly normalized following an additional cell cycle of OPCs before they differentiate. However, we cannot rule out the possibility that ectopic OPCs originating from other rostral and caudal progenitor domains of the neural tube may migrate into the r2-r3 domain and play a role in compensating for the early reduction of ventral oligodendrogenesis.

### *Hoxa2* inactivation results in dorsal expansion of the *Olig2* progenitor domain and increased oligodendrogenesis

To confirm the inhibitory effect of *Hoxa2* on hindbrain oligodendrogenesis, we next analyzed the effect of *Hoxa2* loss of function. At E13.5, *Hoxa2*$^{EGFP-/-}$ mutant embryos showed a dorsally expanded ventricular domain of Olig2 expression, compared with heterozygous littermates (Fig. 4*A*–*D*). Motor neuron specification appeared normal, as indicated by the pattern of Islet1/2 expression (data not shown). In contrast, *Hoxa2*$^{EGFP-/-}$ embryos formed twice as many PDGFRα$^+$ OPCs than controls in the r2d-r4d ventral plate (Fig. 4*E*–*H*). The number of PDGFRα$^+$ OPCs was not altered in r1d, as expected by the lack of *Hoxa2* expression in r1 during normal development. Similar to *Hoxa2* overexpression, *Hoxa2* deletion did not significantly alter OPC migration in the r2d-r4d region, as shown by the similar percentage of migrating OPCs in *Hoxa2*$^{EGFP-/-}$ mutants and *Hoxa2*$^{EGFP+/-}$ controls (percentage of Olig2$^+$ migrating cells ± SEM: r2d-r3d: *Hoxa2*$^{EGFP+/-}$, 20.6 ± 2.8; *Hoxa2*$^{EGFP-/-}$, 14.1 ± 1.6; $p = 0.0690$; r4d: *Hoxa2*$^{EGFP+/-}$, 14.6 ± 1.6; *Hoxa2*$^{EGFP-/-}$, 11.4 ± 2.3; $p = 0.291$; Student's *t* test, $n = 4$). Moreover, at E18.5, *Hoxa2*$^{EGFP-/-}$ mutants showed a similar number of OPCs and mature oligodendrocytes than control mice [mean number of PDGFRα$^+$ cells per area (mm$^2$) ± SEM: r2d: *Hoxa2*$^{EGFP+/-}$ (control), 272.1 ± 65.4; *Hoxa2*$^{EGFP-/-}$, 280.6 ± 119.1; r3d: *Hoxa2*$^{EGFP+/-}$, 340.5 ± 112.2; *Hoxa2*$^{EGFP-/-}$, 309.7 ± 104.8; mean number of CNP$^+$ cells per area (mm$^2$): r2d: *Hoxa2*$^{EGFP+/-}$, 8.9 ± 5.6; *Hoxa2*$^{EGFP-/-}$, 11.2 ± 10.1; r3d: *Hoxa2*$^{EGFP+/-}$, 11.4 ± 10.2; *Hoxa2*$^{EGFP-/-}$, 23.8 ± 24.1]. Thus, the loss of *Hoxa2* function has an early impact on the onset of oligodendrogenesis, which can be compensated at later developmental stages.

*Hoxa2* inhibits ventral oligodendrogenesis by spatially restricting the dorsal extent of oligodendrocyte generation in r2d-r4d territories and thus, ultimately, limiting the size of the Olig2$^+$ domain. Indeed, previous studies showed DV rhombomere patterning defects in *Hoxa2* mutants as early as E10.5 (Davenne et al., 1999). We anticipated that in *Hoxa2*-deficient embryos such DV pattern defects may persist through later stages and have direct consequences on the patterning of the *Olig2* progenitor domain. Thus, we examined the expression of DV patterning genes implicated in oligodendrogenesis and neurogenesis, including *Pax6*, *Nkx2.2*, *Nkx6.1*, and *Ngn2*. In E13.5 *Hoxa2*$^{EGFP-/-}$ mutant embryos, the transcript levels and expression patterns of all these genes were altered in the rostral hindbrain, compared with control heterozygotes (Fig. 5*A*–*L*). Namely, the expression domains of *Nkx2.2* (Fig. 5*A*,*B*,*G*,*H*) and *Olig2* (Fig. 5*G*–*L*) in the r2d-r4d ventral plate were dorsally extended. *Pax6* expression was decreased in r2d-r4d, with a dorsal

←

(*Figure legend continued.*) ***R***, Olig2 expression was weak in highly fluorescent cells (dark arrowheads), while progenitors strongly expressing Olig2 displayed a low level of GFP fluorescence (white arrowheads). r(*n*)d, rhombomere-derived domain. ***G***, r2d, $p = 0.0009$; r3d, $p = 0.0069$; ***H***, r2d, $p = 0.0034$; r3d, $p = 0.0010$; r4d, $p = 0.0193$. $n = 3$ animals of each type. Area, 1 mm$^2$. Scale bars: ***A***, ***B***, ***D***, ***E***, ***J***, ***K***, ***L***, ***N***, ***P***, 100 μm; ***C***, ***F***, ***M***, ***O***, 50 μm; ***Q***, ***R***, 25 μm. *$p < 0.05$; **$p < 0.01$; ***$p < 0.001$.

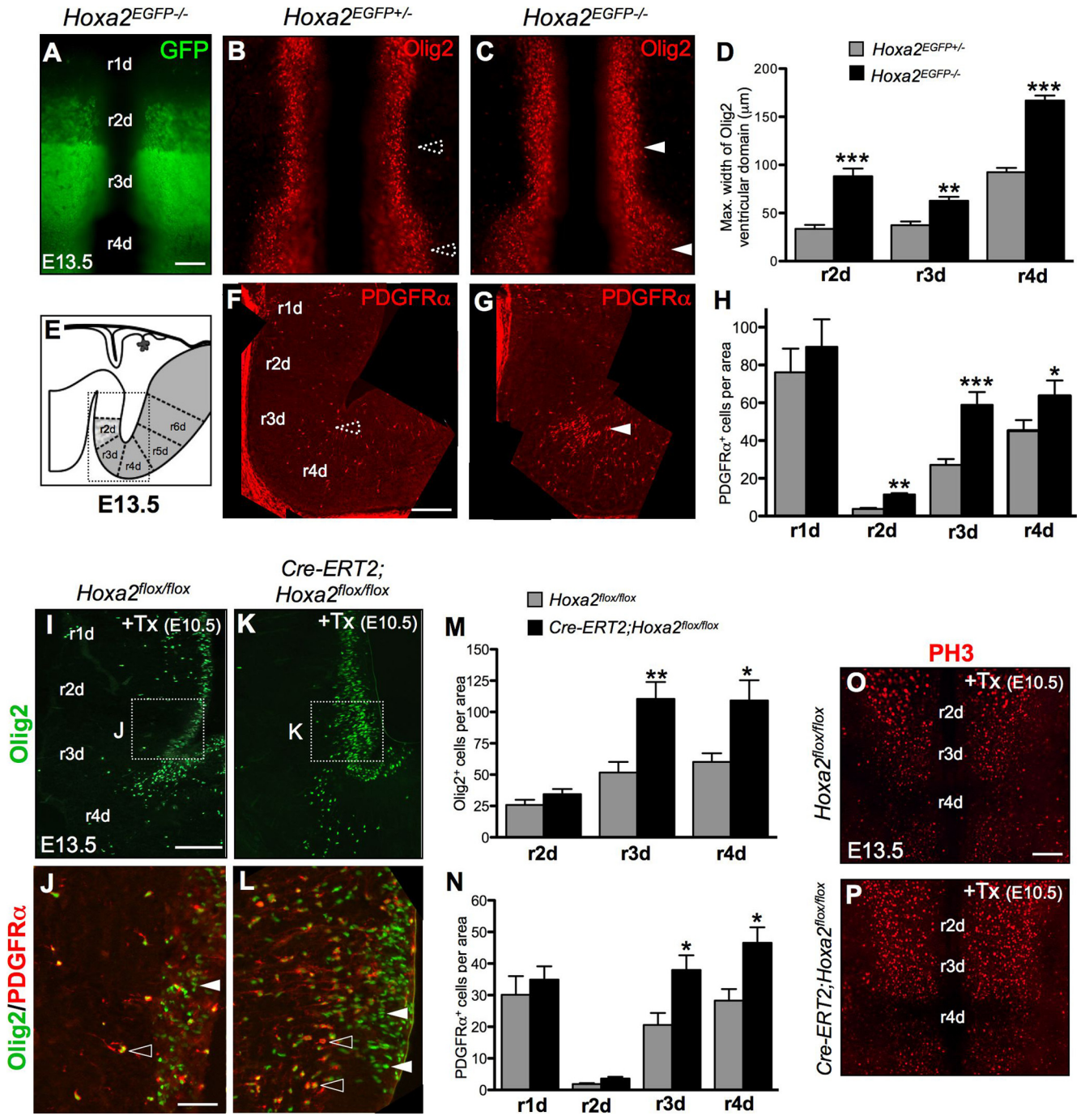


**Figure 4.** *Hoxa2* deletion increases oligodendrogenesis in the rostral hindbrain. ***A–H***, Hindbrain flat-mounts (***A–C***) and sagittal sections (***E–G***) from *Hoxa2*$^{EGFP+/-}$ (***B***, ***F***) and *Hoxa2*$^{EGFP-/-}$ (***A***, ***C***, ***G***) embryos at E13.5, labeled for GFP (green) and Olig2 or PDGFR$\alpha$ (red). *Hoxa2*-deficient mice show an enlarged Olig2$^+$ progenitor domain (***C***, ***D***) and an increased number of PDGFR$\alpha^+$ OPCs (***G***, ***H***) in the basal plate of r2d, r3d, and r4d, compared with controls (***B***, ***F***). ***I–L***, Sagittal sections from Tx-treated *Hoxa2*$^{flox/flox}$ (***I***, ***J***) and *CMV-Cre-ERT2; Hoxa2*$^{flox/flox}$ (***K***, ***L***) embryos, induced at E10.5, sacrificed at E13.5, and immunolabeled for Olig2 (green) and PDGFR$\alpha$ (red). Tx-induced *Hoxa2* knockout embryos display an increased number of Olig2$^+$ (***K***, ***M***) and PDGFR$\alpha^+$ (***L***, ***N***) cells in the basal plate of r3d and r4d, compared with control animals (***I***, ***J***). White and black arrowheads indicate Olig2$^+$ cells and PDGFR$\alpha^+$ cells, respectively, in ***J*** and ***L***. ***O***, ***P***, Hindbrain flat-mounts from Tx-treated *Hoxa2*$^{flox/flox}$ and *CMV-Cre-ERT2; Hoxa2*$^{flox/flox}$ embryos, induced at E10.5 and sacrificed at E13.5, labeled for PH3. Tx-induced *Hoxa2* knockout embryos (***P***) show an increased number of PH3$^+$ cells in the basal plate of r2d-r3d, compared with control mice (***O***). r(*n*)d, rhombomere-derived domain. ***D***, r2d, $p = 0.0009$; r3d, $p = 0.0044$; r4d, $p < 0.0001$; $n = 4$ animals of each type; ***H***, r2d, $p = 0.00397$; r3d, $p = 0.000133$; r4d, $p = 0.0370$; $n = 6$ animals of each type; ***M***, r3d, $p = 0.0014$; r4d, $p = 0.0131$; ***N***, r3d, $p = 0.011$; r4d, $p = 0.036$; $n = 7$ animals of each type. Area, 1 mm$^2$. Scale bars: ***F***, ***G***, ***I***, ***K***, 200 $\mu$m; ***A***--***C***, ***O***, ***P***, 100 $\mu$m; ***J***, ***L***, 80 $\mu$m. *$p < 0.05$; **$p < 0.01$; ***$p < 0.001$.

shift of its ventral border (Fig. 5*C*,*D*,*I*,*J*). Similarly, the ventral border of the Nkx6.1$^+$ domain was shifted dorsally in r2d-r3d (Fig. 5*E*,*F*). The expression levels of the proneural gene *Ngn2* were also reduced in r2d-r4d, with a dorsal extension of its ventral ventricular domain (Fig. 5*K*,*L*). In contrast, no expression abnormalities were observed for Pax3 and Pax7 in the dorsal plate of *Hoxa2*$^{EGFP-/-}$ embryos (data not shown). Thus, *Hoxa2* inhibits the dorsal extension of the *Olig2*$^+$/*Nkx2.2*$^+$ domain in the ventral plate by restricting the dorsoventral extent of bHLH and homeodomain (HD) transcription factors regulating oligodendrogenesis, such as *Pax6*, *Nkx6.1*, and *Ngn2* (Fig. 5*M*,*N*, summary model).

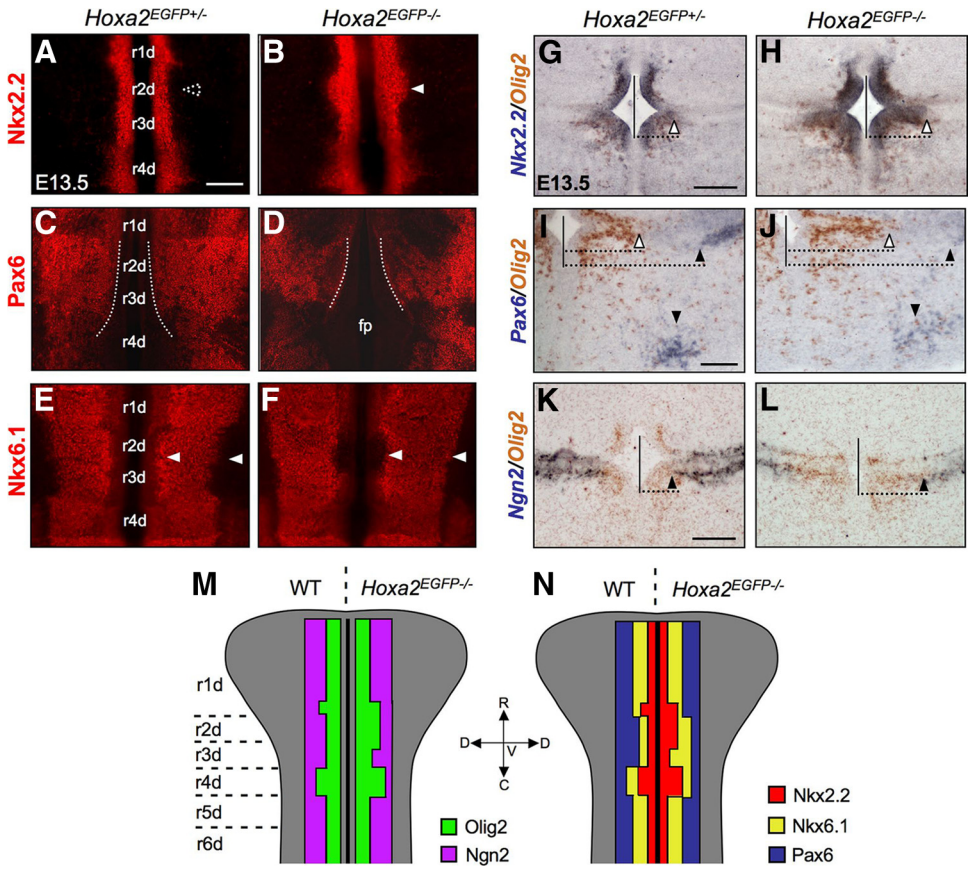


**Figure 5.** Rhombomere-specific alterations of bHLH and HD transcription factors after *Hoxa2* deletion. ***A–F***, Hindbrain flat-mounts from $Hoxa2^{EGFP+/-}$ and $Hoxa2^{EGFP-/-}$ E13.5 embryos immunolabeled with anti-Nkx2.2 (***A***, ***B***), Pax6 (***C***, ***D***), or Nkx6.1 (***E***, ***F***) antibodies. In $Hoxa2^{EGFP-/-}$ mutants, the Nkx2.2$^+$ domain expands more dorsally in r2d (***B***, arrowheads), the Pax6$^+$ domain extends less ventrally (***D***, dotted line), and the Nkx6.1$^+$ domain shows a ventral downregulation and a dorsal expansion in r2d-r3d (***F***, white arrowheads), compared with controls (***A***, ***C***, ***E***). ***G–L***, Double *in situ* hybridizations performed on coronal sections from $Hoxa2^{EGFP+/-}$ and $Hoxa2^{EGFP-/-}$ E13.5 embryos at the r2d-r4d level, labeled for *Olig2* (brown) and either *Nkx2.2* (***G***, ***H***), *Pax6* (***I***, ***J***), or *Ngn2* (***K***, ***L***) (blue) probes. In *Hoxa2*-deficient mice, *Olig2* (***G–J***, white arrowheads) and *Nkx2.2* (***G***, ***H***, white arrowheads) expression domains are expanded dorsally in the ventral plate of r2d-r4d, whereas *Pax6* (***I***, ***J***, black arrowheads) and *Ngn2* (***K***, ***L***, black arrowheads) are ventrally downregulated. ***M***, ***N***, Schematic representations of flat-mounted E13.5 hindbrains indicating alterations of bHLH (***M***) and HD (***N***) transcription factor expression in *Hoxa2*-deficient mice. r(*n*)d, Rhombomere-derived domain; fp, floor plate; R, rostral; C, caudal; V, ventral; D, dorsal. $n = 3$ animals of each type. Scale bars: ***A–F***, 200 $\mu$m; ***G–L***, 100 $\mu$m.

To assess the temporal requirement of *Hoxa2*, we next tested whether increased oligodendrogenesis could be still induced by deleting *Hoxa2* after establishment of RC and DV rhombomere patterning, though before the onset of oligodendrogenesis. A $Hoxa2^{flox}$ allele (Ren et al., 2002) was mated with a Tx-inducible *CMV-βactin-Cre-ERT2* line (Santagati et al., 2005). As hindbrain oligodendrogenesis starts at ~E12.5, and it takes ~36–48 h after Tx treatment to induce efficient CreERT2-mediated excision, we administered Tx by oral gavage to E10.5 pregnant *CMV-Cre-ERT2;*$Hoxa2^{flox/flox}$ homozygous mutant females (see Materials and Methods). At E13.5, Tx-induced *CMV-Cre-ERT2;*$Hoxa2^{flox/flox}$ mutants showed an increased number of Olig2$^+$ and PDGFRα$^+$ OPCs in the basal plate of r3d-r4d, compared with control Tx-treated $Hoxa2^{flox/flox}$ embryos, similar to $Hoxa2^{EGFP-/-}$-deficient mice (Fig. 4*I–N*). This phenotype was due to an increased cell proliferation in the ventricular zone, as shown by the greater number of PH3$^+$ cells compared with controls (Fig. 4*O*,*P*; mean number of PH3$^+$ cells per area (mm$^2$) ± SEM: $Hoxa2^{flox/flox}$, 30.6 ± 1.6; *CMV-Cre-ERT2;* $Hoxa2^{flox/flox}$, 42.4 ± 1.9; $p < 0.0001$, Student's *t* test, $n = 4$). In r2d-r3d territories, PH3$^+$ cells located in the ventral and lateral plates displayed an increase of PH3$^+$/PDGFRα$^+$ OPCs (percentage of PH3$^+$/PDGFRα$^+$ cells/total PDGFRα$^+$ cells ± SEM: $Hoxa2^{flox/flox}$, 1.2 ± 0.7; *CMV-Cre-ERT2;* $Hoxa2^{flox/flox}$, 4.2 ± 0.2; $p = 0.0034$; Student's *t* test, $n = 4$). Immunostaining for cleaved caspase-3 showed no differences in OPC survival between mutants and control mice (no caspase-3$^+$ cells detected in the r2d-r3d domain of controls and *Hoxa2* mutants). Thus, *Hoxa2* function is required at least until the onset of oligodendrogenesis.

In summary, our functional gain-of-function and loss-of-function data provide converging evidence that *Hoxa2* is normally required to spatially and quantitatively restrict the generation of ventral Olig2$^+$ progenitors in the rostral hindbrain.

### *Hoxb2* promotes hindbrain oligodendrogenesis

Previous studies established that *Hoxb2* has an important role in neuronal patterning in the ventral hindbrain (Barrow and Capecchi, 1996; Davenne et al., 1999; Pattyn et al., 2003). Indeed, in the *Nkx2.2*$^+$ domain of ventral r4d, *Hoxb2* contributes to facial motor neuron generation by maintaining high expression levels of the paired HD factor Phox2b, which, in turn, suppresses serotonergic (5HT) fate (Pattyn et al., 2003). To evaluate the role of *Hoxb2* in ventral oligodendrogenesis, we examined the oligodendroglial phenotype of *Hoxb2* loss-of-function mutants, $Hoxb2^{del/del}$ (see Materials and Methods). At E13.5, $Hoxb2^{del/del}$ hindbrain flat-mounts displayed a reduced

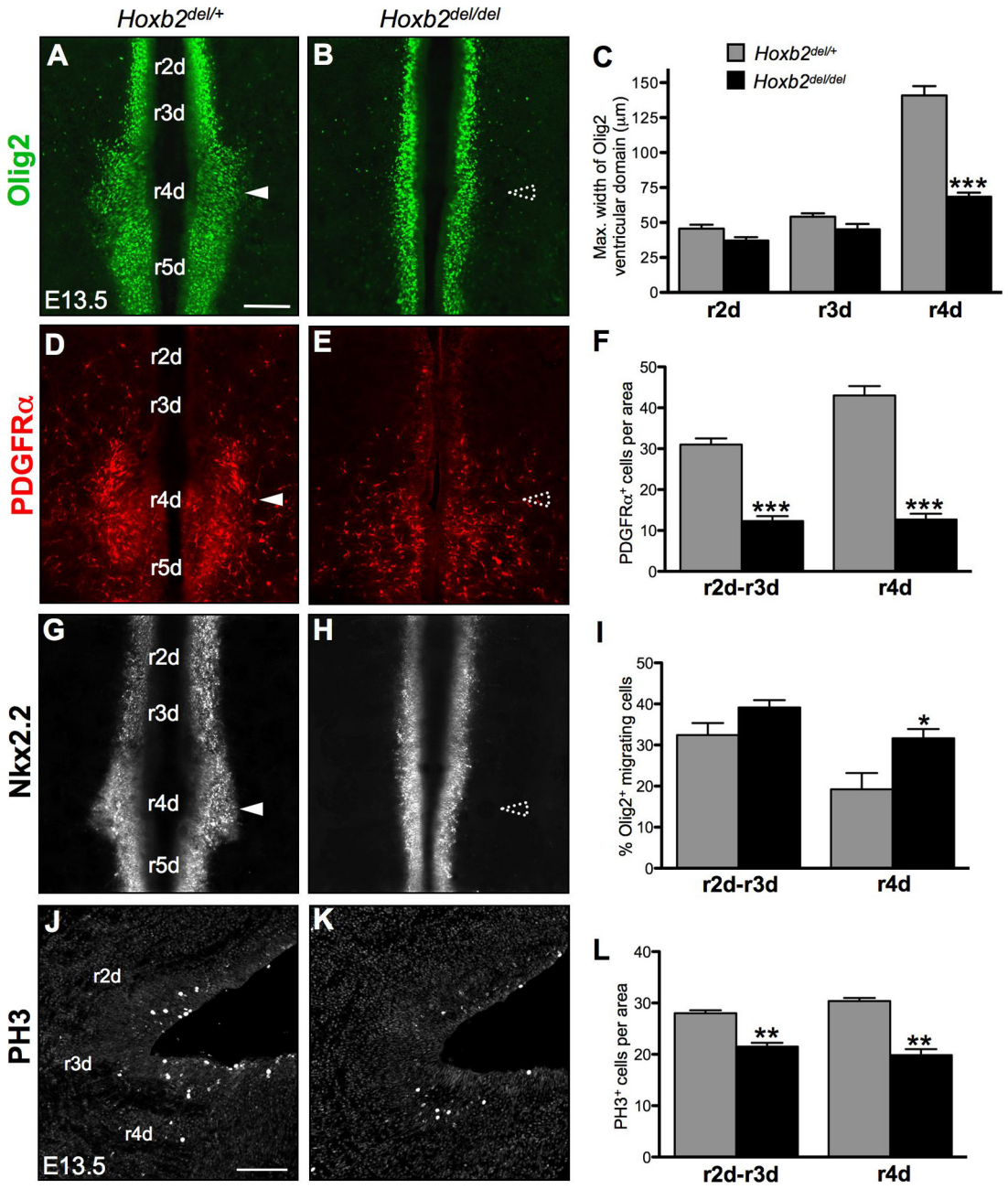


**Figure 6.** *Hoxb2* deletion decreases oligodendrogenesis. ***A–I***, Flat-mounted hindbrains from *Hoxb2*$^{del/+}$ (***A***, ***D***, ***G***) and *Hoxb2*$^{del/del}$ (***B***, ***E***, ***H***) embryos at E13.5, analyzed after immunolabeling with anti-Olig2 (green), anti-PDGFR$\alpha$ (red), and anti-Nkx2.2 (white) antibodies. *Hoxb2* deletion results in a reduction of the dorsoventral extension of Olig2 (***A–C***) and Nkx2.2 (***G***, ***H***) ventricular domains in r4d, as well as in a decreased number of PDGFR$\alpha^+$ cells (***D–F***) in r2d-r4d. *Hoxb2*-null embryos also show a higher percentage of Olig2$^+$ migrating cells in r4d, compared with control animals (***I***). ***J–L***, Sagittal sections from *Hoxb2*$^{del/+}$ (***J***) and *Hoxb2*$^{del/del}$ (***K***) mice at E13.5, labeled for PH3. *Hoxb2*$^{del/del}$ embryos display a reduced number of proliferating cells in r2d-r4d. r(*n*)d, rhombomere-derived domain. ***C***: r4d, $p < 0.0001$; ***F***: r2d-r3d, $p = 0.0007$; r4d, $p = 0.0004$; ***I***: r4d, $p = 0.0256$; ***L***: r2d-r3d, $p = 0.0025$; r4d, $p = 0.0013$; $n = 4$ animals of each type. Area, 1 mm$^2$. Scale bars, 100 $\mu$m. *$p < 0.05$; **$p < 0.01$; ***$p < 0.001$.

Olig2$^+$ domain in r4d (Fig. 6*A–C*) and a decreased number of ventral PDGFR$\alpha^+$ OPCs (Fig. 6*D–F*), compared with control embryos. The Nkx2.2 expression domain, which is dorsally enlarged at the level of r4d in wild-type embryos, compared with r2d-r3d, was also reduced in size (Fig. 6*G*,*H*). Unlike *Hoxa2*, *Hoxb2* appears to positively regulate cell proliferation in the prepontine and pontine regions (r3d-r4d), as shown by the reduced number of PH3$^+$ cells present in *Hoxb2*$^{del/del}$ mutants, compared with wild-type littermates (Fig. 6*J–L*). *Hoxb2* might also regulate OPC migration, since we observed an increased percentage of migrating Olig2$^+$ cells in the r4d of *Hoxb2*-deficient mice (Fig. 6*I*). At E18.5, we found no apparent differences in the number of PDGFR$\alpha^+$ OPCs and mature CNP$^+$ oligodendrocytes in the rostral hindbrain between *Hoxb2*$^{del/del}$ mutants and controls (data not shown). Thus, the decrease in the number of OPCs formed at E13.5 has been compensated and did not result in a reduced population of mature oligodendrocytes.

In summary, the lack of *Hoxb2* results in a phenotype opposite to that of *Hoxa2* inactivation. Namely, unlike *Hoxa2*, *Hoxb2* promotes expansion of OPCs, especially in r4d, where it also promotes extended facial motor neuron generation (Pattyn et al., 2003).

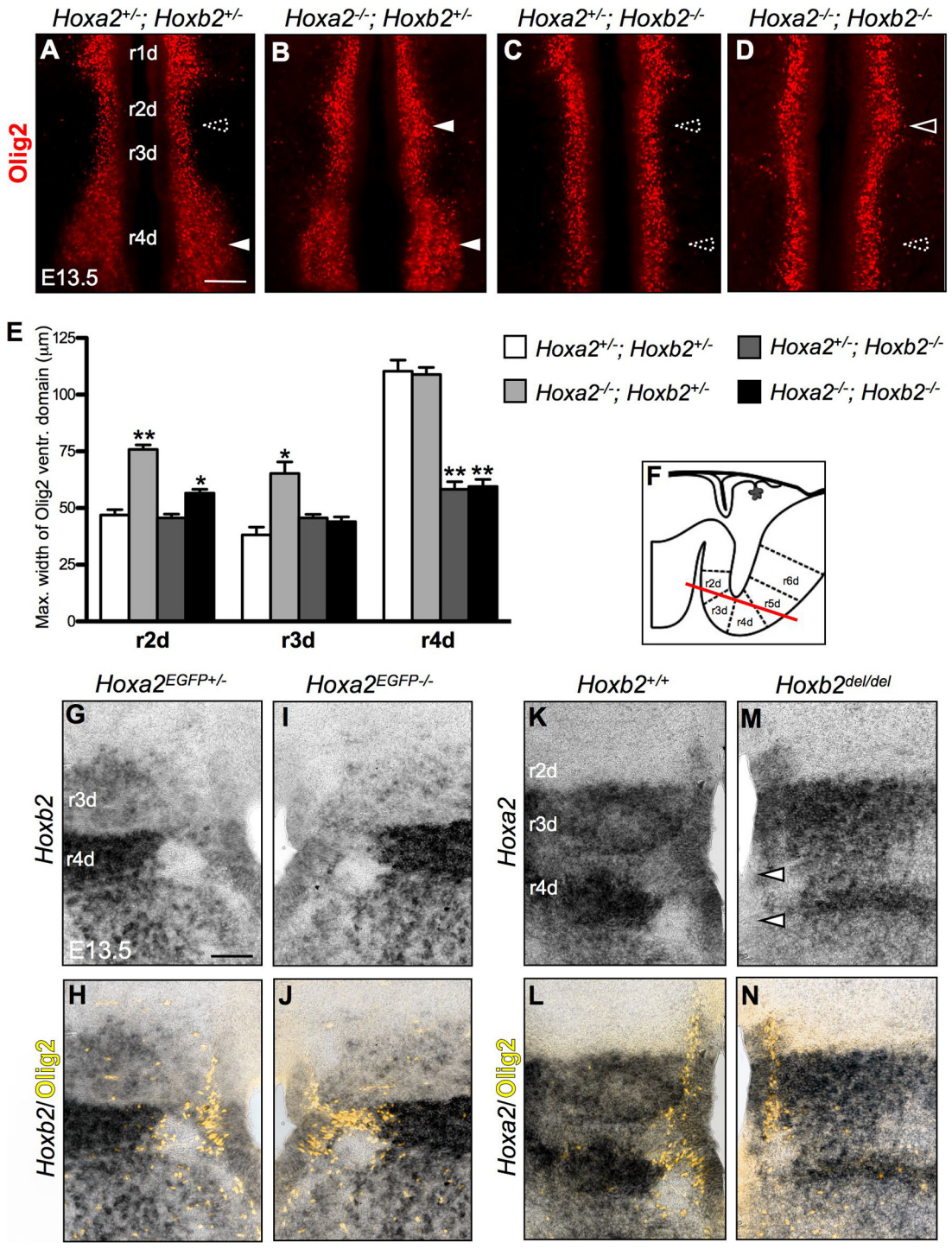


**Figure 7.** Cross-regulatory interaction between *Hoxa2* and *Hoxb2* in hindbrain oligodendrogenesis. ***A–E***, Hindbrain flat-mounts from $Hoxa2^{+/-}/Hoxb2^{+/-}$ (***A***), $Hoxa2^{-/-}/Hoxb2^{+/-}$ (***B***), $Hoxa2^{+/-}/Hoxb2^{-/-}$ (***C***), and $Hoxa2^{-/-}/Hoxb2^{-/-}$ (***D***) E13.5 embryos analyzed after immunolabeling with anti-Olig2 antibody. The dorsoventral extension of $Olig2^{+}$ ventricular domain in each rhombomere is indicated in ***E***. Compared with double heterozygous control animals (***A***), $Hoxa2^{-/-}/Hoxb2^{-/-}$ embryos (***D***) show (1) an enlarged $Olig2^{+}$ ventricular domain in r2d, but not in r3d, where this effect is compensated by the loss of *Hoxb2*; (2) a reduced $Olig2^{+}$ ventricular domain in r4d, like in $Hoxa2^{+/-}/Hoxb2^{-/-}$ (***C***) or $Hoxb2^{-/-}$ mutants, independently of the loss of *Hoxa2*, indicating that *Hoxb2* dominates *Hoxa2* for the control of *Olig2* expression. ***G–N***, *In situ* hybridizations for *Hoxb2* and *Hoxa2* followed by Olig2 immunolabeling, performed on coronal sections from $Hoxa2^{EGFP}$ (***G–J***) and $Hoxb2^{del}$ (***K–N***) E13.5 mutants, respectively. Sections are localized as indicated in ***F***. *Hoxb2* expression pattern was similar between $Hoxa2^{EGFP-/-}$ mutants and $Hoxa2^{EGFP+/-}$ controls (***G***, ***I***). In contrast, *Hoxa2* expression in the ventricular $Olig2^{+}$ domain of r4d was downregulated in $Hoxb2^{-/-}$ mutants (***M***, arrowheads). ***E***, r2d: $Hoxa2^{+/-}/Hoxb2^{+/-}$ versus $Hoxa2^{-/-}/Hoxb2^{+/-}$, $p = 0.0027$; $Hoxa2^{+/-}/Hoxb2^{+/-}$ versus $Hoxa2^{-/-}/Hoxb2^{-/-}$, $p = 0.0184$; r3d: $Hoxa2^{+/-}/Hoxb2^{+/-}$ versus $Hoxa2^{-/-}/Hoxb2^{+/-}$, $p = 0.0262$; r4d: $Hoxa2^{+/-}/Hoxb2^{+/-}$ versus $Hoxa2^{+/-}/Hoxb2^{-/-}$, $p = 0.0038$; $Hoxa2^{+/-}/Hoxb2^{+/-}$ versus $Hoxa2^{-/-}/Hoxb2^{-/-}$, $p = 0.0035$; $n = 3$ animals of each type. Scale bars, 100 μm. $^{*}p < 0.05$; $^{**}p < 0.01$; $^{***}p < 0.001$.

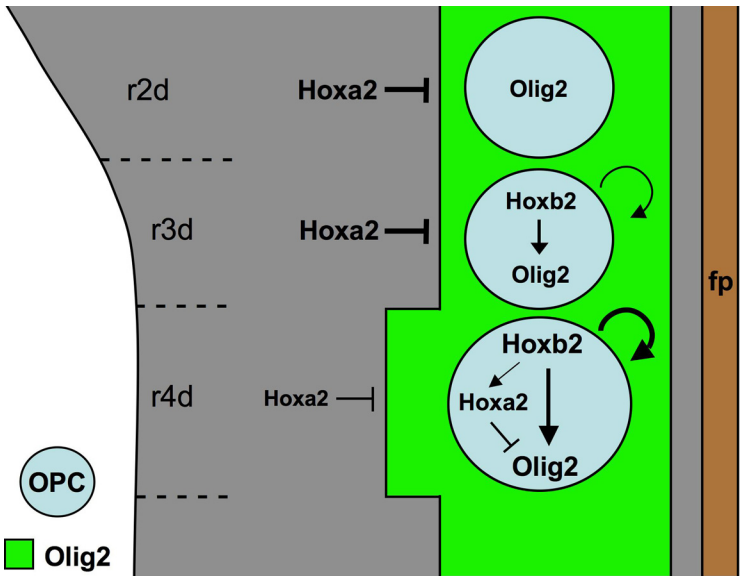


**Figure 8.** Working model of *Hox* PG2 action in oligodendrogenesis of rostral hindbrain. *Hoxa2* and *Hoxb2* have opposing effects on hindbrain oligodendrogenesis. *Hoxa2* acts predominantly in the environment of Olig2 progenitors, especially in the Pax6 domain, where it represses *Olig2* expression and limits the dorsal extension and the size of *Olig2* progenitor domain. This effect is prominent in the r2d-r3d domain. *Hoxb2* promotes oligodendrogenesis and increases proliferation of Olig2$^+$ progenitors and OPCs in the r3d-r4d domain. This effect is especially robust in ventral r4d, where *Hoxb2* controls *Hoxa2* expression in the progenitor domain. r(*n*)d, rhombomere-derived domain; fp, floor plate.

### Cross-regulatory interaction between *Hoxa2* and *Hoxb2* in hindbrain oligodendrocyte patterning

The phenotypes of single *Hoxa2* and *Hoxb2* mutants indicate opposing roles for *Hoxb2* and *Hoxa2* in hindbrain oligodendrogenesis, suggesting that a net balance between *Hoxa2* and *Hoxb2* expression levels in the Olig2$^+$ domain may modulate the number of OPCs generated in each rhombomere posterior to r1. To test this hypothesis, we analyzed the pattern of Olig2$^+$ progenitors and PDGFR$\alpha^+$ OPCs in compound *Hoxa2*/*Hoxb2* mutants and their littermates at stage E13.5 (Fig. 7*A–E*). In r2d, where *Hoxa2*, but not *Hoxb2*, is expressed, *Hoxa2*$^{-/-}$/*Hoxb2*$^{-/-}$ mutants showed, as expected, a similar dorsal expansion of the Olig2$^+$ domain as in single *Hoxa2*$^{-/-}$ mutants. Interestingly, in r3d, the loss of *Hoxb2* in double *Hoxa2*$^{-/-}$/*Hoxb2*$^{-/-}$ homozygotes was sufficient to prevent the increased oligodendrogenesis displayed by single *Hoxa2*$^{-/-}$ mutants. Thus, the Olig2 expression pattern in r3d suggests that the promoting effect of *Hoxb2* on oligodendrogenesis is dominant upon the inhibitory action of *Hoxa2*. This was further supported by the finding that in r4d of *Hoxa2*$^{-/-}$/*Hoxb2*$^{-/-}$ mutants, the reduction of the Olig2$^+$ ventral domain (Fig. 7*D*) was similar to that of *Hoxa2*$^{+/-}$/*Hoxb2*$^{-/-}$ (Fig. 7*C*) and single *Hoxb2*$^{-/-}$ mutants (Fig. 6*B*), while single *Hoxa2*$^{-/-}$ mutants displayed a twofold increase of Olig2$^+$ cells in this domain (Fig. 4*C*). The Olig2 expression pattern in r4d confirms that Hoxb2 antagonizes and dominates Hoxa2 in the regulation of rhombomere-specific oligodendrogenesis.

To determine whether Hoxa2 and Hoxb2 each regulates each other's expression, we examined the hindbrain expression pattern of *Hoxa2* in *Hoxb2* mutants and, reciprocally, of *Hoxb2* in *Hoxa2*-deficient embryos (Fig. 7*F–N*). The *Hoxb2* expression pattern was not changed in *Hoxa2*$^{EGFP-/-}$ mutants, compared with *Hoxa2*$^{EGFP+/-}$ controls (Fig. 7*G–J*). In contrast, in *Hoxb2*$^{-/-}$ mutants, *Hoxa2* was significantly downregulated in the ventricular Olig2$^+$/Nkx2.2$^+$ progenitor domain of r4d (Fig. 7*K–N*, arrowheads). This is in agreement with a direct regulatory role for Hoxb2 in maintaining *Hoxa2* expression levels in r4 (Lampe et al., 2008) and explains the similar oligodendrocyte phenotypes of single *Hoxb2*$^{-/-}$ and compound *Hoxa2*$^{-/-}$/*Hoxb2*$^{-/-}$ mutants in the ventral r4d domain. Therefore, *Hoxa2* and *Hoxb2* likely act together in ventral oligodendrocyte progenitors, at least in r4d, exerting opposite modulatory effects on the molecular processes regulating OPC specification and proliferation.

## Discussion

In this study, we found that *Hox* PG2 genes have opposing roles in the regulation of oligodendrocyte generation and patterning in the rostral hindbrain. In the spinal cord, Hox homeoproteins are expressed by oligodendroglial cells (Nicolay et al., 2004a,b; Booth et al., 2007), raising the possibility that they may confer RC identity to oligodendrocytes. However, in the spinal cord of *Hoxa2*-deficient mice, no anomalies were detected in the number, migration, and differentiation of OPCs (Nicolay et al., 2004b). Nonetheless, many *Hox* genes are coexpressed at the level of the spinal cord, thus providing the potential for functional redundancy that may mask the involvement of individual Hox factors. To overcome the redundancy pitfall and investigate the possible involvement of Hox PG2 factors in oligodendrogenesis, we focused on the rostral hindbrain where *Hoxa2* and *Hoxb2* perform their main functional role. Indeed, we provide evidence that *Hoxa2* and *Olig2* expression levels are inversely correlated in progenitor cells, and that Hoxa2 might be involved in restricting the ventral domain of oligodendrocyte specification. From E12.5 to E14.5, ventral oligodendrogenesis is induced in prepontine and pontine territories in progenitors expressing low levels of *Hoxa2*. In mice conditionally overexpressing *Hoxa2* in Olig2$^+$ progenitors, the size of the ventral Olig2 domain is reduced, especially in r2d-r3d territories. The inhibition of oligodendrogenesis induced by *Hoxa2*-overexpression may occur independently of environmental cues, as it is not only evident in the hindbrain but also, more generally, in other brain regions, such as the ventral forebrain. In *Hoxa2*-deficient mice, there is a dorsal expansion of the ventral Olig2$^+$/Nkx2.2$^+$ domain resulting in increased oligodendrogenesis. This is in part due to the loss of *Hoxa2* expression at the ventral border of the abutting *Pax6*$^+$ ventricular domain, where Hoxa2 is normally highly expressed, and to ectopic recruitment of *Olig2*$^+$ progenitors. Like *Hoxa2*, *Hoxb2* is expressed in the ventral plate, but, unlike *Hoxa2*, it promotes *Olig2* expression, as indicated by the narrowing of the *Olig2* domain in the r4d ventral plate of *Hoxb2*-deficient mice and double *Hoxa2*$^{-/-}$/*Hoxb2*$^{-/-}$ mutants. The coexpression of *Hoxa2* and *Hoxb2* transcripts in the ventral Nkx2.2$^+$ ventricular domain and the downregulation of *Hoxa2* expression in the r4d ventral ventricular domain of *Hoxb2*$^{-/-}$ mutants, suggest a feedforward cross-regulatory inhibitory mechanism between Hoxb2 and Hoxa2 to regulate the number and the local production of oligodendrocytes in ventral progenitor cells of the rostral hindbrain.

Figure 8 proposes a schematic model to explain how *Hox* PG2 genes can regulate rostral hindbrain oligodendrogenesis. High *Hoxa2* expression levels are required to maintain the ventral bor-

der of *Pax6* expression, where it contributes to repress *Olig2* activation in ventricular progenitors. *Pax6* may directly bind to the *Olig2* promoter and repress *Olig2* expression, as recently reported in stem/progenitor cells (Jang and Goldman, 2011). Moreover, Olig2$^+$ progenitors may be specified at the dorsal edge of the *Nkx2.2*$^+$ domain at a developmental stage when *Hoxa2* expression levels are declining. This is suggested by the observation that forced maintenance of high *Hoxa2* expression levels in Olig2$^+$ cells, as in *Olig2-tva-Cre*;*ROSA*$^{(lox\text{-}stop\text{-}lox)Hoxa2}$ mice, inhibits oligodendrogenesis. Regarding *Hoxb2*, our data show that it promotes progenitor cell proliferation in the ventroalar plate and acts in *Olig2*$^+$ ventral progenitors to increase oligodendrogenesis, likely by counteracting *Hoxa2*-mediated inhibition in r3d and r4d. However, it is noteworthy that in the ventral r4d *Nkx2.2*$^+$ domain Hoxb2 is also involved in the maintenance of high *Hoxa2* expression levels, which, in turn, inhibit the generation of *Olig2*$^+$ progenitors. Such a transcriptional cross-regulation of Hoxb2 on *Hoxa2* may be direct, since a *Hoxa2* r4-specific enhancer regulated by Hoxb1 and/or Hoxb2 has been previously identified (Tümpel et al., 2007; Lampe et al., 2008). Concerning Hoxb2 regulation of *Olig2* expression, it could be direct, by binding onto *Olig2* promoter, or indirect, by modulating the expression of effectors of signaling molecules regulating *Olig2* expression, including those induced by SHH.

The alterations of DV patterning observed in the rostral hindbrain of *Hox* PG2 mutants suggest that *Hox* PG2 genes regulate cell fate choices within several progenitor domains along the DV axis (Davenne et al., 1999). The *Nkx2.2*$^+$ progenitor domain of r2d and r3d, but not r4d, generates the serotonergic lineage before the onset of oligodendrogenesis (Pattyn et al., 2003). We found that the number and distribution of 5HT$^+$ cells was not modified in *Hoxa2*-deficient or in *Hoxa2*-overexpressing mice, compared with controls, suggesting that OPCs are not produced at the expense of serotonergic progenitors and that *Hoxa2* does not regulate serotonergic versus oligodendroglial cell fate balance in *Nkx2.2*-expressing progenitors (data not shown). Dorsally to the *Nkx2.2*$^+$/*Olig2*$^+$ ventral domain, the *Pax6* ventricular domain includes a ventral subset of progenitors committed to generate astroglial cells (Hochstim et al., 2008). In *Hoxa2*-deficient embryos, a normal number of glial cells expressing Sox9 form in the rostral hindbrain (data not shown). Since Sox9 is a common marker for immature oligodendroglial and astroglial cells (Stolt et al., 2003), this suggests that fewer astrocytes and more OPCs are produced compared with wild-type mice. The excess of OPCs generated in the ventral plate of these mutants may be produced at the expense of astrocytes derived from the reduced *Pax6* domain. In contrast, the gain of ventral oligodendrogenesis in *Hoxa2*$^{EGFP-/-}$ embryos is not associated with a loss or a reduction of dorsal oligodendrogenesis, which later derives from the *Pax3*/*Pax7*/*Gsh1* ventricular domain (Vallstedt et al., 2005), as no alterations of Pax3 and Pax7 expression patterns were detected in the hindbrain of these mutants.

The observations reported here indicate that rostral hindbrain oligodendrogenesis develops in the ventral plate with a defined spatiotemporal pattern involving segment-specific subpopulations of oligodendroglial progenitors of different size and distribution. Hoxa2 and Hoxb2 appear to contribute to the dorsoventral patterning of ventricular progenitors and to regulate spatially restricted proliferation of progenitor and precursor cells in the ventroalar plate. Although additional effects on the migration of OPCs cannot be ruled out, especially for *Hoxb2* in r4d, *Hox* PG2 genes appear to be mainly required at an early stage of regional OPC generation from ventral progenitor cells. Moreover, *Hoxa2* and *Hoxb2* do not apparently contribute to regulate oligodendrocyte differentiation, since neither *Hoxa2* nor *Hoxb2* mutations altered the number of CNP$^+$ oligodendrocytes in the rostral hindbrain. The action of *Hox* PG2 genes is temporally restricted and the number of OPCs produced at the onset of oligodendrogenesis in *Hoxa2* or *Hoxb2* mutants is rapidly normalized before birth. In *Hoxa2* gain-of-function and *Hoxb2*-deficient mutants, the reduced number of ventricular progenitors and early born OPCs are likely compensated by an additional cell cycle of OPCs before they differentiate. In *Hoxa2* loss-of-function mutants, the elimination of extra numerous OPCs born at E13.5 probably result from the competition between OPCs to use the limited amount of PDGF-A available in the environment, since PDGF-A-driven cell survival controls override proliferation for determining the final number and distribution of mature oligodendrocytes (Calver et al., 1998).

*Hox* PG2 genes participate in rostral hindbrain oligodendrogenesis, but may also regulate OPC production and behavior in more caudal regions of the neural tube, where such genes are expressed. It is very likely that, in addition to *Hoxb2*, other *Hox* genes may modulate the repressing effect of *Hoxa2* to control the ventral expression of *Olig2* and the size of the ventral oligodendrogenic domain. A more complete picture of *Hox* gene function in oligodendroglial development would require global and inducible *Hox* deletion. Hox proteins require common Pbx cofactors to achieve their function (Moens and Selleri, 2006). Conditional deletion of Pbx (pre-B cell leukemia transcription) factors in OPCs may provide useful genetic models to better evaluate the importance of *Hox* regulation in brainstem and spinal cord oligodendrogenesis.

In patients with multiple sclerosis, not only is the distribution of demyelinating lesions extremely variable, but the capacity of remyelination varies depending on the lesioned territory. For instance, it has been reported that cortical lesions remyelinate much more efficiently than periventricular plaques (Patrikios et al., 2006; Albert et al., 2007). This local vulnerability of myelin raises the possibility that it could be related to regional populations of oligodendrocytes with different myelin vulnerabilities and/or repair abilities. Investigating the molecules conferring the regional identity of oligodendrocytes may thus have an important impact on therapeutic strategies aimed at favoring or enhancing myelin repair following white matter lesions at spatially restricted locations in the CNS. In this respect, it may be of particular interest to examine whether a differential expression of either HOXA2 or HOXB2 in multiple sclerosis lesions in the hindbrain may account for the different capacity of some lesions to repair or not, and whether manipulating HOX PG2 factors may contribute to increase myelin repair.

## References

Albert M, Antel J, Brück W, Stadelmann C (2007) Extensive cortical remyelination in patients with chronic multiple sclerosis. Brain Pathol 17:129–138. CrossRef Medline

Barrow JR, Capecchi MR (1996) Targeted disruption of the Hoxb-2 locus in mice interferes with expression of Hoxb-1 and Hoxb-4. Development 122:3817–3828. Medline

Booth J, Nicolay DJ, Doucette JR, Nazarali AJ (2007) Hoxd1 is expressed by oligodendroglial cells and binds to a region of the human myelin oligodendrocyte glycoprotein promoter in vitro. Cell Mol Neurobiol 27:641–650. CrossRef Medline

Cai J, Qi Y, Hu X, Tan M, Liu Z, Zhang J, Li Q, Sander M, Qiu M (2005) Generation of oligodendrocyte precursor cells from mouse dorsal spinal cord independent of Nkx6 regulation and Shh signaling. Neuron 45:41–53. CrossRef Medline

Calver AR, Hall AC, Yu WP, Walsh FS, Heath JK, Betsholtz C, Richardson

WD (1998) Oligodendrocyte population dynamics and the role of PDGF in vivo. Neuron 20:869–882. CrossRef Medline

Davenne M, Maconochie MK, Neun R, Pattyn A, Chambon P, Krumlauf R, Rijli FM (1999) Hoxa2 and Hoxb2 control dorsoventral patterns of neuronal development in the rostral hindbrain. Neuron 22:677–691. CrossRef Medline

Davies JE, Miller RH (2001) Local sonic hedgehog signaling regulates oligodendrocyte precursor appearance in multiple ventricular zone domains in the chick metencephalon. Dev Biol 233:513–525. CrossRef Medline

Di Lullo E, Haton C, Le Poupon C, Volovitch M, Joliot A, Thomas JL, Prochiantz A (2011) Paracrine Pax6 activity regulates oligodendrocyte precursor cell migration in the chick embryonic neural tube. Development 138:4991–5001. CrossRef Medline

Dupé V, Davenne M, Brocard J, Doll é P, Mark M, Dierich A, Chambon P, Rijli FM (1997) In vivo functional analysis of the Hoxa-1 3′ retinoic acid response element (3′RARE). Development 124:399–410. Medline

Dymecki SM (1996) Flp recombinase promotes site-specific DNA recombination in embryonic stem cells and transgenic mice. Proc Natl Acad Sci U S A 93:6191–6196. CrossRef Medline

Fogarty M, Richardson WD, Kessaris N (2005) A subset of oligodendrocytes generated from radial glia in the dorsal spinal cord. Development 132:1951–1959. CrossRef Medline

Geisen MJ, Di Meglio T, Pasqualetti M, Ducret S, Brunet JF, Chedotal A, Rijli FM (2008) Hox paralog group 2 genes control the migration of mouse pontine neurons through Slit-Robo Signaling. PLoS Biol 6:e142. CrossRef Medline

Gu H, Zou YR, Rajewsky K (1993) Independent control of immunoglobulin switch recombination at individual switch regions evidenced through Cre-loxP-mediated gene targeting. Cell 73:1155–1164. CrossRef Medline

Hochstim C, Deneen B, Lukaszewicz A, Zhou Q, Anderson DJ (2008) Identification of positionally distinct astrocyte subtypes whose identities are specified by a homeodomain code. Cell 133:510–522. CrossRef Medline

Hunt P, Gulisano M, Cook M, Sham MH, Faiella A, Wilkinson D, Boncinelli E, Krumlauf R (1991) A distinct Hox code for the branchial region of the vertebrate head. Nature 353:861–864. CrossRef Medline

Jang ES, Goldman JE (2011) Pax6 expression is sufficient to induce a neurogenic fate in glial progenitors of the neonatal subventricular zone. PLoS One 6:e20894. CrossRef Medline

Káradóttir R, Hamilton NB, Bakiri Y, Attwell D (2008) Spiking and nonspiking classes of oligodendrocyte precursor glia in CNS white matter. Nat Neurosci [Erratum (2008) 11:851] 11:450–456. CrossRef Medline

Kessaris N, Fogarty M, Iannarelli P, Grist M, Wegner M, Richardson WD (2006) Competing waves of oligodendrocytes in the forebrain and postnatal elimination of an embryonic lineage. Nat Neurosci 9:173–179. CrossRef Medline

Kim SU, McMorris FA, Sprinkle TJ (1984) Immunofluorescence demonstration of 2′:3′-cyclic-nucleotide 3′-phosphodiesterase in cultured oligodendrocytes of mouse, rat, calf and human. Brain Res 300:195–199. Medline

Lampe X, Samad OA, Guiguen A, Matis C, Remacle S, Picard JJ, Rijli FM, Rezsohazy R (2008) An ultraconserved Hox-Pbx responsive element resides in the coding sequence of Hoxa2 and is active in rhombomere 4. Nucleic Acids Res 36:3214–3225. CrossRef Medline

Lumsden A, Krumlauf R (1996) Patterning the vertebrate neuraxis. Science 274:1109–1115. CrossRef Medline

Moens CB, Selleri L (2006) Hox cofactors in vertebrate development. Dev Biol 291:193–206. CrossRef Medline

Narita Y, Rijli FM (2009) Hox genes in neural patterning and circuit formation in the mouse hindbrain. Curr Top Dev Biol 88:139–167. CrossRef Medline

Nicolay DJ, Doucette JR, Nazarali AJ (2004a) Hoxb4 in oligodendrogenesis. Cell Mol Neurobiol 24:357–366. CrossRef Medline

Nicolay DJ, Doucette JR, Nazarali AJ (2004b) Early stages of oligodendrocyte development in the embryonic murine spinal cord proceed normally in the absence of Hoxa2. Glia 48:14–26. CrossRef Medline

Noll E, Miller RH (1993) Oligodendrocyte precursors originate at the ventral ventricular zone dorsal to the ventral midline region in the embryonic rat spinal cord. Development 118:563–573. Medline

Nyabi O, Naessens M, Haigh K, Gembarska A, Goossens S, Maetens M, De Clercq S, Drogat B, Haenebalcke L, Bartunkova S, De Vos I, De Craene B, Karimi M, Berx G, Nagy A, Hilson P, Marine JC, Haigh JJ (2009) Efficient mouse transgenesis using Gateway-compatible ROSA26 locus targeting vectors and F1 hybrid ES cells. Nucleic Acids Res 37:e55. CrossRef Medline

Ono K, Fujisawa H, Hirano S, Norita M, Tsumori T, Yasui Y (1997) Early development of the oligodendrocyte in the embryonic chick metencephalon. J Neurosci Res 48:212–225. Medline

Oury F, Murakami Y, Renaud JS, Pasqualetti M, Charnay P, Ren SY, Rijli FM (2006) Hoxa2 and rhombomere dependent development of the mouse facial somatosensory map. Science 313:1408–1413. CrossRef Medline

Pasqualetti M, Ren SY, Poulet M, LeMeur M, Dierich A, Rijli FM (2002) A Hoxa2 knockin allele that expresses EGFP upon conditional Cre-mediated recombination. Genesis 32:109–111. CrossRef Medline

Patrikios P, Stadelmann C, Kutzelnigg A, Rauschka H, Schmidbauer M, Laursen H, Sorensen PS, Brück W, Lucchinetti C, Lassmann H (2006) Remyelination is extensive in a subset of multiple sclerosis patients. Brain 129:3165–3172. CrossRef Medline

Pattyn A, Vallstedt A, Dias JM, Samad OA, Krumlauf R, Rijli FM, Brunet JF, Ericson J (2003) Coordinated temporal and spatial control of motor neuron and serotonergic neuron generation from a common pool of CNS progenitors. Genes Dev 17:729–737. CrossRef Medline

Pringle NP, Yu WP, Guthrie S, Roelink H, Lumsden A, Peterson AC, Richardson WD (1996) Determination of neuroepithelial cell fate: induction of the oligodendrocyte lineage by ventral midline cells and sonic hedgehog. Dev Biol 177:30–42. CrossRef Medline

Ren SY, Pasqualetti M, Dierich A, Le Meur M, Rijli FM (2002) A Hoxa2 mutant conditional allele generated by Flp- and Cre-mediated recombination. Genesis 32:105–108. CrossRef Medline

Richardson WD, Kessaris N, Pringle N (2006) Oligodendrocyte wars. Nat Rev Neurosci 7:11–18. CrossRef Medline

Rodríguez CI, Buchholz F, Galloway J, Sequerra R, Kasper J, Ayala R, Stewart AF, Dymecki SM (2000) High-efficiency deleter mice show that FLPe is an alternative to Cre-loxP. Nat Genet 25:139–140. CrossRef Medline

Rowitch DH (2004) Glial specification in the vertebrate neural tube. Nat Rev Neurosci 5:409–419. CrossRef Medline

Rowitch DH, Kriegstein AR (2010) Developmental genetics of vertebrate glial-cell specification. Nature 468:214–222. CrossRef Medline

Santagati F, Minoux M, Ren SY, Rijli FM (2005) Temporal requirement of Hoxa2 in cranial neural crest skeletal morphogenesis. Development 132:4927–4936. CrossRef Medline

Schüller U, Heine VM, Mao J, Kho AT, Dillon AK, Han YG, Huillard E, Sun T, Ligon AH, Qian Y, Ma Q, Alvarez-Bylla A, McMahon AP, Rowditch DH, Ligon KL (2008) Acquisition of granule neuron precursor identity is a critical determinant of progenitor cell competence to form Shh-induced medulloblastoma. Cancer Cell 14:123–134. CrossRef Medline

Spassky N, Goujet-Zalc C, Parmantier E, Olivier C, Martinez S, Ivanova A, Ikenaka K, Macklin W, Cerruti I, Zalc B, Thomas JL (1998) Multiple restricted origin of oligodendrocytes. J Neurosci 18:8331–8343. Medline

Spassky N, Heydon K, Mangatal A, Jankovski A, Olivier C, Queraud-Lesaux F, Goujet-Zalc C, Thomas JL, Zalc B (2001) Sonic hedgehog-dependent emergence of oligodendrocytes in the telencephalon: evidence for a source of oligodendrocytes in the olfactory bulb that is independent of PDGFRalpha signaling. Development 128:4993–5004. Medline

Stolt CC, Lommes P, Sock E, Chaboissier MC, Schedl A, Wegner M (2003) The Sox9 transcription factor determines glial fate choice in the developing spinal cord. Genes Dev 17:1677–1689. CrossRef Medline

Sugimori M, Nagao M, Bertrand N, Parras CM, Guillemot F, Nakafuku M (2007) Combinatorial actions of patterning and HLH transcription factors in the spatiotemporal control of neurogenesis and gliogenesis in the developing spinal cord. Development 134:1617–1629. CrossRef Medline

Timsit S, Martinez S, Allinquant B, Peyron F, Puelles L, Zalc B (1995) Oligodendrocytes originate in a restricted zone of the embryonic ventral neural tube defined by DM-20 mRNA expression. J Neurosci 15:1012–1024. Medline

Tripathi RB, Clarke LE, Burzomato V, Kessaris N, Anderson PN, Attwell D, Richardson WD (2011) Dorsally and ventrally derived oligodendrocytes have similar electrical properties but myelinate preferred tracts. J Neurosci 31:6809–6819. CrossRef Medline

Tümpel S, Cambronero F, Ferretti E, Blasi F, Wiedemann LM, Krumlauf R (2007) Expression of Hoxa2 in rhombomere 4 is regulated by a conserved cross-regulatory mechanism dependent upon Hoxb1. Dev Biol 302:646–660. CrossRef Medline

Vallstedt A, Klos JM, Ericson J (2005) Multiple dorsoventral origins of oli-

godendrocyte generation in the spinal cord and hindbrain. Neuron 45: 55–67. CrossRef Medline

Wegner M (2008) A matter of identity: transcriptional control in oligodendrocytes. J Mol Neurosci 35:3–12. CrossRef Medline